Study of Strongly Coupled Systems via Probe Brane Constructions

Han-Chih Chang

A dissertation
submitted in partial fulfillment of the
requirements for the degree of

Doctor of Philosophy

University of Washington

2014

Reading Committee:

Andreas Karch, Chair

Ann Nelson

Anton Andreev

Program Authorized to Offer Degree:
UW Department of Physics, Particle Theory Group

University of Washington

Abstract

Study of Strongly Coupled Systems via Probe Brane Constructions

Han-Chih Chang

Chair of the Supervisory Committee:
Professor Andreas Karch
Department of Physics

In this thesis, we present our study towards better understanding of the strongly coupled systems with extra matter content in the fundamental representation of some prescribed global symmetry group in the quenched approximation, with the toolkit of holography via a probe brane construction. We will recapitulate the main result of our works, published in the following journals:

- Chapter 2 is mostly adapted from our work, "Minimal Submanifolds asymptotic to $AdS_4 \times S^2$ in $AdS_5 \times S^5$", Journal of High Energy Physics, vol.1404, p.037, 2014 [1].

  We map out the first-order phase transitions associated with the bottom-up model describing the zero-temperature phases for the coupled phase between two two-dimensional defects stacked parallel in a four-dimensional ambient spacetime, dual to the presence of spontaneous symmetry breaking of the individual ultraviolet flavor symmetries associated with the double heterostructure of the defect layers.

- Chapter 3 is mostly adapted from our work, "The Novel Solutions of Finite-Density D3/D5 Probe Brane System and Their Implications for Stability", in collaboration with Prof. Andreas Karch, Journal of High Energy Physics, vol.1210, p.060, 2014 [2].

  We discover a novel set of solutions of the probe brane system consisting of N_f D5-

probe branes embedded in the near-horizon geometry generated by N_c D3-branes, with the D5 worldvolume $U(1)$ gauge fields turned on, holographically dual to a supersymmetric defect field theory at finite density in non-trivial vacua.

- Chapter 4 is mostly adapted from our work, "Entanglement Entropy for Probe Branes", in collaboration with Prof. Andreas Karch, Journal of High Energy Physics, vol.1401, p.180, 2014 [3].

  We give a prescription for calculating the entanglement entropy in holographic probe brane systems by systematically taking the leading order backreaction of the probe brane into account. We validate our method by comparing to exact results in solvable toy models, and also determine the entanglement entropies for a sphere and a strip in the top-down D3/D7 and D3/D5 system.

The unifying theme of these works is to better understand the novel quantum phases realized using holography. Specifically, for the defect conformal systems, we unearth and quantify the phase trasition diagram (Chapter 2), and novel supersymmetric vacua (Chapter 3) in the top-down model of the D3/D5 probe brane system. For further quantify various non-Fermi quantum liquid phases realized through the holographical probe brane construction, we then propose and verify the method to include the backreaction due to the probe branes at the leading order (Chapter 4), which can potentially be used to detect topological phase transitions. Finally, we conclude and briefly comment on future directions in Chapter 5.

TABLE OF CONTENTS

Page

LIST OF FIGURES

Figure Number Page

ACKNOWLEDGMENTS

The author wishes to express sincere appreciation to the Particle Theory Group in the Physics Department of University of Washington, from which he is given the privileged opportunity to explore freely the vast realm of Theoretical High Energy Physics, with the extraordinary guidance from Prof. Andreas Karch, Ann Nelson, David Kaplan, Steve Ellis, Steve Sharpe, and Lawrence Yaffe.

DEDICATION

to my parents.

Chapter 1

INTRODUCTION

1.1 Origin: the Effective Field Theory Paradigm and Beyond

Quantum field theories (QFTs), as the natural framework emerging from unifying the principles of quantum mechanics, special relativity and cluster decomposition [4, 5], have been proved to be extremely fruitful descriptions of theoretical physics. After the conceptual overhaul led by the advent of the Wilsonian renormalization group flow (RG flow), nowadays we understand QFTs as effective field theories (EFTs), a paradigm that disperses the often-quoted confusion associated with the renormalization procedure of the UV divergences from the perturbative loop expansions. Moreover, the viewpoint from EFTs also opens up its modern applications in the vast realms of many-body systems, from high energy particle physics [4], condensed matter physics [6, 7], to the large-scale cosmology [8, 9], all of which are successfully understood and modeled with this common EFT framework.

Nevertheless, despite the powerful concept of separation of scale, which ensures QFTs are the correct language for low-energy processes (irrespective of any high-energy physics lurking beyond), still we may quite legitimately seek to augment this agnostic EFT viewpoint by categorizing all possible UV-completion mechanisms. This line of inquiry naturally leads to the following two different directions of focus: 1) within QFT framework, we might gain more understanding by classifying all possible fixed points of the Wilsonian RG flows on the field theory space, realized as conformal field theories (CFTs)[1], of which

[1] Notice that we have restricted ourselves in the context of relativistic QFTs. However, even within relativistic QFTs, it is a nontrivial statement that a relativistic QFT at the RG flow fixed point, which is tautologically scale-invariant, will be also conformal-invariant, as the former lacks the generators of the special conformal transformations that the latter posses (a point vehemently emphasized in Migdal's vivid recollection of the history of conformal field theory [10]). Still, up to the writing of this thesis, the counterexamples (*ie.* being scale-invariant but not conformal-invariant) all admit unphysical behaviors, and hence it is a long unsolved question to unearth the missing link for inferring conformal invariance from

the most elusive ones are the strongly coupled versions; 2) beyond QFT framework, we might go beyond the usual foundations of QFT. For example, string theory [12, 13, 14, 15] manages to abolish the foundations of particles (0-dimensional objects) and manifestly local interactions, and postulate the 1-dimensional objects as the elementary degree of freedom, *ie.* strings. This framework, as we will briefly review below, not only provides a UV-complete description for formulation of quantum gravity (QG), is capable of UV-completion of the grand unification theories (GUTs), but also gives us a handle to understand the zoo of QFTs and the associated surprising equivalence among seemingly different QFTs, as realized by the brane construction [16].

In fact, all the above considerations are manifest in the standard model of particle physics. As it currently stands, the standard model is still the most accurate theory that humankind has ever constructed. With all its global symmetries realized as accidental symmetries of the standard model Lagrangian, its versatilities are all naturally explained as the ubiquitous IR consequence from the chosen gauge groups and matter content, as expected from the EFT framework [17, 18]. However, two above-mentioned inquiries can be embedded as following. Admittedly the standard model is described by a trivial IR fixed point, but it is not UV-complete in this present formulation. Not only does the $U(1)_Y$ gauge group suffer from the Landau pole problem[2], the $U(1)_Y \times SU(2)_L$ gauge groups fail to comply with the usual lattice UV-completion[3], but also there is the most conspicuous absence of gravity in the standard model[4]. Therefore, one might proceed through the above-mentioned

---

scale invariance. A recent work has pointed out that unitary itself might be enough to close the logical gap: See [11] and the detail analysis within.

[2] It is noteworthy to point out the observed Higgs mass renders the problem of Landau pole above the Plank scale, hence the standard model, as it currently stands, is phenomenologically robust at low energy, and *a priori* there can be no new physics till QG scale. However, another viewpoint augmenting EFT philosophy is the notion of naturalness, and in this viewpoint the current standard model suffers from the hierarchy problem, *ie.* the "unprotected" quantum correction of the mass parameter of the elementary spin-0 Higgs field. Nevertheless, due to the nature of this more aesthetically/psychologically inspired notion, together with the failure to observe the natural supersymmetric partners at Large Hadron Collider (LHC) up to the writing of this thesis, there have been calls to re-evaluate the utilities of naturalness and the associated hierarchy problem.

[3] The current formulation of lattice gauge theories can not be performed to the electro-weak sector due to obstruction from the chiral matter content.

[4] More precisely, it is the lack of control over the UV behaviors (above the Plank scale) of QG in the EFT framework due to the dimensionful Newton's constant.

two lines of inquiries. 1) Within QFT framework, one might seek a GUT realization that can accommodate the standard model as its low-energy description, but itself being UV-complete at high energy. Being asymptoticly free is one feasible approach, and there are also proposals of utilizing strongly coupled QFTs for dynamically (and hence naturally) explaining different scales observed in nature. As for the lack of control of QG, the proposal of strongly coupled QFTs, *ie.* the asymptotic safety program, is also another potential candidate within the field theory rescue. Moreover, even without asking UV-completion/QG that many physicists consider as far-fetching, the quark-gluon plasma (QGP) discovered at the Relativistic Heavy Ion Collider (RHIC) of the Brookhaven National Lab (BNL) already urges us to come up with some theoretical method capable of probing the real-time, finite-density properties of strongly coupled many-body systems, which currently are still beyond the reach of the usual non-perturbative lattice calculation. 2) Beyond QFT framework, one might consider the complete reformulation as realized by the heterotic superstring theories, $SO(32)$ or $E_8 \times E_8$, and construct the associated string phenomenology [19], embedding the standard model within, and hence solving various above-mentioned problems altogether.

Surprisingly, these two separate lines of inquiry, of strongly coupled CFTs and of the UV-completed QG as the superstring theory, are reunited by the notion of Anti-de Sitter/Conformal Field Theory (AdS/CFT) correspondence, also known as the gauge-string duality [20, 21, 22, 23]. In retrospect, various endeavors have hinted at such a duality. From the field theory side, we have already discovered the emergent notions of stringy phenomena through the large-N expansion. From the gravity side, we also have already discovered the holography principle as inspired by the area law of black hole entropy. With all other earlier endeavors and tantalizing hints, it was culminated in 1997 when Maldacena [20] articulated the conjecture of the existence of an exact (quantum-)equivalence between $N = 4$ supersymmetric Yang-Mills (SYM) gauge theory in 4-dimensional Minkowski spacetime, and Type IIB superstring theory on $AdS_5 \times S^5$ background. As the nature of this conjecture as being a strong-weak duality (reviewed later), it is difficult to prove directly this equivalence, for this itself is equivalent to solving the difficult strongly coupled dynamics. Nonetheless, ever since the original proposal, a huge amount of indirect but nontrivial tests have been performed, all found to be supporting this conjecture, and the notion of gauge-string duality has also

been further extended and applied beyond the original conjectured systems, and hence itself becomes a useful toolbox for building intuitions for strongly coupled phenomena [24].

Given the abundant evidence accumulated in favor of the gauge-string duality, various "folklores" are also being formulated/conjectured in order to retrospectively motivate or understand this conjecture. We find two such "folklores", albeit vague and borderline philosophical, still serve some pedagogical purposes, and hence are worth mentioning at least to the newcomers to the field. We will therefore collect these two "folklores" in the following [24]. On the field theory side, there is the folklore of "geometrizing"the renormalization group flow. Associated with one chosen QFT, let us first picture a stack of infinite EFTs, each EFT being the intermediate theory along the line transversed by the RG flow of the original QFT. We also picture the whole stake of EFTs being ordered from UV to IR renormalization scales, *ie.* high-energy EFTs sitting higher in the stake, and vice versa. Notice now that any such "intermediate" EFT, living at some slice of the stack, is nonlocal due to the lack of fine resolution from the loss of higher momentum modes along the RG flow. However, being an EFT itself, this intermediate EFT will "holographically" capture the entire low-energy physics as recorded by the lower "bulk" stack of all other EFTs sitting beneath. "Holographically" in the sense that this EFT is located at the boundary of the entire lower "bulk" stack. Still, we must remember that this whole stack of infinite EFTs is actually nothing but just a very redundant description of the original QFT. Combined with the notion that the RG flow is only an explicit function of coupling constants (hence being implicit functions of RG scale), it will be tempting to "construct", or "sew" together this whole stack of EFTs into a single bulk theory, as an alternative (redundant) manifestation of the original QFT, a description that is nonlocal and holographic by construction. On the other hand, on the gravity/string theory side, one might choose to stress the foundational issue associated with a theory with the dynamically fluctuating metric. With the bulk metric itself being fluctuating, we lose the notion of unambiguously specifying local bulk insertions in advance, since we don't know how to specify a metric-invariant[5] meaning

[5] Notice this is entirely different from being metric-covariant, which is just the reparametrization invariance, a redundancy of our description among different coordinates. We can simply eliminate this redundancy either by brutally adapting some gauge fixing condition (and later checking the consistence belaboringly), or by more carefully moding out the associated gauge volume using the usual Faddev-Popov

of bulk points, a perquisite for bulk operator insertions in this functional-integral formalism. However, such an obstruction is moot with boundary insertions: with the boundary present, the well-posedness of the functional-integral formalism already requires us to specify the boundary condition (chosen so the functional integration-by-part holds), hence no fluctuating boundary metric and no ambiguity of specifying boundary points. Therefore, we might argue that one should formulate any theory of dynamic bulk metric entirely in terms of a prescribed boundary metric, and only obtain boundary correlation functions as physical objects. Admittedly, the above "folklores" themselves are not sufficient to pinpoint the exact dual descriptions as later clarified by the gauge-string duality. Nevertheless, we will like to stress that these two "folklores" highlight the crucial properties of both sides of the duality, of the technical observations in the field theory side and of the fundamental arguments in the string theory sides, that still serve as relevant notions for later developments, such as the holographic renormalization group flow and the QG entanglement entropy.

1.2 Birth, Decline and Reemergence of Stringy Descriptions: Problems of the Strong Interaction, and the Large-N Expansion

In retrospect, the connection between string theory and strongly coupled gauge theories has also been lurking since the very conceptions of each other in the strong interaction [25]. Originally born out as the dual-resonance model, string theory was first constructed to explain the observed Regge trajectory, upon which the masses of strongly-interacting particle/resonances are related to their angular momenta. However, since the advent of Quantum Chromodynamics (QCD) for successfully explaining the Bjorken scaling in the deep inelastic scattering at the SLAC National Accelerator Laboratory, QCD has been established as the underlying physics responsible for the strong interaction, and the above-mentioned earlier success of string theory is qualitatively understood as the success of the effective description capturing some stringy excitations within the QCD spectrum. Figuratively, we

---

procedure. In any case, the above-mentioned obstruction is not concerning the gauge-orbit direction but the physical direction in the field space, changing the proper length between bulk points. Therefore, given the bulk proper length cannot be fixed *a priori*, there appears no way to differentiate, or "anchor", any points in the bulk to begin with. This renders the arguments of bulk n-point correlation functions ill-defined.

now understand, in the language of QCD, the putative strings are the QCD color-electric flux tubes, with all its stringy properties descending from the QCD confinement due to the condensation of QCD color-magnetic monopoles, *ie.* the dual Meissner effect proposed by 't Hooft and Mandelstam [26]. Given the success accumulated by QCD, the research in string theory hence fell out of the mainstream physics, remained dormant and only later rekindled after it was shown capable of formulating not only the UV-completed models of QG (anomaly cancellations), but also the observed chiral nature of the standard model content as embedded in the grand unification theories (GUTs).

However, the triumph of QCD at high energy, as consolidated in Bjorken scaling and asymptotic freedom, also harbingers the same problem that we nowadays are still struggling with, *ie.* the low energy strongly coupled regime of QCD. The basic idea can be understand by recalling the notion of dimensional transmutation. The classical freedom to specify the dimensionless coupling constant $\alpha_{\rm bare}$ in the classical Lagrangian, after quantization and renormalization procedure, is transmuted into the freedom of specifying a physical dimensional scale Λ_{QCD}[6], only later to be determined with the experimental data. In QCD, the phenomena of asymptotic freedom (the coefficient b_1, in footnote 6, being negative) translates into the so-called "IR slavery", *ie.* the increase of the resummed effective coupling constant[7] $\alpha_{\rm eff}(\mu)$ as we probe into the lower energy physics at scale μ. However, when the resummed effective coupling constant becomes of order 1, the usual lower-order loop calculations lose their utility, and we are forced to adopt other non-perturbative approaches, such as lattice QCD or chiral field theory (χFT), to answer various important IR physical questions, such as the QCD vacuum structure, the meson/baryon spectra, and chiral condensate.

Nevertheless, a surprising breakthrough was achieved by 't Hooft in 1973 [27, 28] that strangely carries a flavor of the stringy description. In view of the QCD dimensional transmutation, hence the lack of a small parameter for perturbative expansion suitable for all

---

[6] Albeit that the physical scale Λ_{QCD} is built out of the arbitrary sliding scale μ and the associated renormalized coupling $\alpha(\mu)$, as $\Lambda_{\text{1-Loop}} = \mu e^{+\frac{1/b_1}{\alpha(\mu)}}$ in one loop.

[7] Here we adopt the EFT language, hence deploying the renormalization-group improved perturbation to maximize the utilities of perturbative expansion.

energy regimes, 't Hooft instead decides to promote the QCD gauge group $SU(3)$ into $SU(N)$, and expands the correlation functions/amplitude in a double expansion of $1/N$ and the properly rescaled coupling constant g^2N (as we will justify later), and only sets $N = 3$ in the end[8]. Furthermore, this expansion turns out to admit a geometric interpretation that coincides with the some 2-dimensional "worldsheet" expansion, and retrospectively foretells the nontrivial connection of gauge theory and string theory revealed only 24 years later by Maldacena.

To see this, let us first considering the following action:

$$S = \frac{1}{g^2}\int dx^4(-\frac{1}{4}F^{a\mu\nu}F^a_{\mu\nu}) + \int dx^4 \sum_f \bar{\psi}^f(i\gamma^\mu D_\mu - m)\psi_f, \tag{1.1}$$

with a being the adjoint representation index of local $SU(N)$ gauge group, f being the flavor index of the possible global symmetry group, μ, ν being the spin-1 4-vector index with the spinor indices suppressed. Notice we have adopted the rescaled definition of gauge fields, $D_\mu \equiv \partial_\mu + A_\mu$, therefore automatically solving the constrain relating the gauge coupling constant renormalization Z_g with the wavefunction renormalization Z_A due to the Ward identity from gauge invariance. As argued already by 't Hooft, to render the large-N expansion relevant to the physical case of $N = 3$, we should demand that the rescaled β function to be non-trivial in the large-N limit. Recall the 1-loop beta function of $SU(N_c)$-QCD coupled vectorially to N_f Dirac fermions in the fundamental representation, in the dimensional regularization/$\overline{\text{MS}}$ subtraction scheme:

$$\mu\frac{d}{d\mu}g(\mu) = -\left(\frac{11}{3}N_c - \frac{2}{3}N_f\right)\frac{g(\mu)^3}{16\pi^2} + \mathcal{O}(g^5). \tag{1.2}$$

Therefore, 't Hooft argues it is physical to fix the large-N scaling of the gauge coupling constant as $g \propto \frac{1}{\sqrt{N}}$, or in other words, we should hold $\lambda_{\text{'t Hooft}} \equiv g^2N$ (also know as the

[8] Expanding in $\frac{1}{N} = \frac{1}{3}$ may cast doubts in the validity of the approximation, but it is a well-known wisecrack of Witten [28] that one may want to recall the QED expansion parameter as $e \approx 0.3028$ from $\alpha_{QED} = \frac{e^2}{4\pi} \approx \frac{1}{137}$, given e and $\frac{1}{N}$ are the proper expansion parameters used in the respective perturbative expansion, for both excluding the phase factor from the kinematics. Hence it is indeed fair to say doubts should be cast in both cases *a priori* before one calculates the associated phase factor from kinematics. In QED, this phase factor turns out to be large, $\frac{1}{16\pi^2}$, as indicated below through a Lorentz-invariant example, hence providing the better controls over the perturbative expansion,

$$\int \frac{dp^4}{(2\pi)^2}f(p^2) = \frac{1}{16\pi^2}\Big(\int dx\, x f(x)|_{x\to p^2}\Big).$$

't Hooft coupling) fixed and then expand around $\frac{1}{N}$. This assignment leads to an overall factor of N in front of the Lagrangian of the gauge fields, hence the gluon propagator being proportional to $\frac{1}{N}$ (2-pt insertions $\propto N$), with the 3-pt and 4-pt interaction insertions being proportional to N. With the help of the double-line notation, one can check that we only need to include a factor of N for every closed loop. Therefore, for a Feynman diagram constructed within the pure gluon sector, with V_G number of 3-pt and 4-pt gluon interaction insertions, I_G number of gluon propagators, and L_G number of closed loops, the corresponding amplitude will carry the large-N scaling of

$$N^{V_G - I_G + L_G}.$$

However, if we instead construct a triangularization of the 2-dimensional surface Σ corresponding to this Feynman diagram, by identifying the propagators as its edges, the interaction insertions as its vertices, and any summed loops as its faces, this same factor is then also admitting geometrical interpretation, as being the associated Euler characteristic of Σ, $N^{2-2g} = N^{\chi(\Sigma)}$ with g being the numbers of the handle thereof. In this way, the large-N expansion has the interpretation as an alternative expansion in terms of all possible topology of some putative 2-dimensional surfaces. To include fermion matter content in the fundamental representation, we need to rescale the fermion field as $\psi \to \psi\sqrt{N}$, hence the large-N scaling assignments for fermion propagators and fermion interaction insertions are the same as those of gluons, with only the caveat that the fermion loop, due to its single line nature, now lacks the associated factors of N. Over all, one can check that it leads to N^{2-2g-b}, with b being the number of fermion loop or the boundary of the putative worldsheet [29].

It is indeed quite surprising that, simply starting from a physically motivated large-N scaling assignment, the perturbative expansion/Feynman diagrams can be reorganized, irrespective of the energy regime, in terms of the topology of some underlying 2-dimensional surfaces that are not even manifestly associated with the high energy Lagrangian description. In fact, even though one might rightfully question the convergence of this reorganization, or the utilities of any information extracted in this limit (for *a priori* they can disappear once we set $\frac{1}{N}$ to $\frac{1}{3}$), studies have nonetheless correlated various phenomenological nuclear

phenomena with their large-N counterparts, as clearly reviewed in [28] and the vast literatures within. Given such a conceptually suggestive and phenomenologically successful description, it is tantalizing to expect there may be some hidden stringy description that is equivalent to the point-particle, QFT description. As we will review in the next section, the gauge-string duality indeed realize such an expectation.

1.3 Genesis of the First Clearest Example of AdS/CFT Duality: D-brane Duality, Decoupling Limit, and $\mathcal{N} = 4$ SYM in Minkowski Space vs. Type IIB String Theory on $AdS_5 \times S^5$ Background

Two major revolutions have shaped the way we understand the modern superstring theory today [25]: The first revolution is when Green and Schwarz demonstrated that the consistency constraint of anomaly cancellation is indeed achievable within the superstring framework, singling out 5 consistent superstring theories as the only possible candidates for the UV-completed QG[9]. However, this disjoint scenario quickly changed with the second revolution led by Witten, building upon various string dualities, and we now understand these 5 different superstring theories are nothing but different limits of one single underlying 11-dimensional theory called M-theory.

Central to this understanding is the notion of Dq-branes [12, 30, 31, 32], and we can understand them in the context of perturbative open-string theory. Recall that in the usual perturbative open-string theory, Dq-branes manifest themselves as the $(q+1)$-dimensional hypersurfaces upon which the open strings can end, where we choose the Dirichlet boundary condition to construct the associated mode functions for open strings. Due to the associated breaking of target spacetime translation invariance (except for the omnipresent D9-branes), initially the study of Dq-branes are mostly for intellectual curiosities. Nonetheless, it was later shown, through explicit scattering calculations, that these hypersurfaces also carry the Ramond-Ramond (RR) charges, and hence they should be identified with the known black q-brane solutions already existing in the closed-string supergravity. Such an identification opens the floodgates of various duality between the 5 different superstring theories, and

[9] More promisingly are the heterotic superstring theories, as they also admit the chiral matter contents observed in the nature/manifested in the standard model

decisively lays the foundation upon which the modern gauge-string duality is built, first constructed by Maldacena. We will collect the relevant information mostly from the review of Aharony *et al.* [23].

The original proposal of Maldacena is built on the dual description of a stack of coincident N_c D3-branes in the (9+1)-dimensional Minkowski target spacetime, in terms of either open- or closed-strings. On the one hand, the open-string description of this system consists of the following three parts: 1) A far-way region, asymptotic to flat Minkowski spacetime, where closed strings propagate away from the branes, 2) A low-energy worldvolume region due to the open strings bounded and propagating on the worldvolume of coincident N_c D3-branes and 3) An intermediate region where the open strings and closed strings interact and scatter close to the branes. Taking a low-energy decoupling limit, *ie.* the Maldacena limit, we can reduce this system into two decoupled sectors, with 1) Type IIB closed string theory on $(9+1)$-Minkowski target spacetime, and 2) The low-energy worldvolume theory of the coincident N_c D3-branes, *ie.* $\mathcal{N}=4$ $U(N_c)$ SYM gauge theory in $(3+1)$-Minkowski spacetime, with the gauge coupling given by

$$g^2 = 4\pi g_s, \tag{1.3}$$

with g_s being the string interaction strength, $g_s = e^{\langle\Phi(\infty)\rangle}$ as the vacuum expectation value of the dilaton field at infinity. On the other hand, consider the closed-string description of this same system, upon which the open-string description of N_c D3-branes is replaced with the (closed-string) Type IIB supergravity solutions, including the black-3-brane background metric and the associated background N_c-unit RR 5-form flux turned on:

$$ds^2 = f^{-\frac{1}{2}}(-dt^2 + {dx_1}^2 + {dx_2}^2 + {dx_3}^2) + f^{\frac{1}{2}}(dr^2 + r^2 d\Omega_5{}^2) \tag{1.4}$$

$$F_5 = (1+*)dt \wedge dx_1 \wedge dx_2 \wedge dx_3 \wedge d(f^{-1}) \tag{1.5}$$

$$f \equiv 1 + \frac{R^4}{r^4}$$

$$R^4 \equiv 4\pi g_s \alpha'^2 N_c \tag{1.6}$$

In this description, we have instead only closed strings, propagating at 1) A far-away region asymptotic to the (9+1)-Minkowski spacetime, 2) A throat region asymptotic to $AdS_5 \times S^5$

spacetime, and 3) A crossover region interpolating the two. Notice that we can once again adopt the Maldacena limit, eliminating the crossover region, however in this case this limit cannot truncate out the stringy states in the throat region, given that the automatic redshift effect renders those stringy states invisible from the far-away region. In the end, we are left within also two decoupled regions as 1) Type IIB closed string theory on $(9+1)$-Minkowski spacetime, and 2) Type IIB closed string theory on $AdS_5 \times S^5$ spacetime and N_c-unit RR 5-form flux.

Therefore, we see the consequence of the exact equivalence[10] of the open- and closed-string descriptions of D3-branes is the advertised exact equivalence of $\mathcal{N} = 4$ $U(N_c)$ SYM gauge theory in $(3+1)$-Minkowski spacetime and Type IIB closed string theory on background of $AdS_5 \times S^5$ spacetime and N_c-unit RR 5-form flux, originally refereed to as the AdS/CFT correspondence. Asides from this surprising duality between gauge theory and string theory, under this duality the strongly coupled regime is also mapped into the weakly coupled regime of the dual theory. To better quantify this strong-weak nature of the AdS/CFT duality, we can ask what is the range of parameters that we can approximate Type IIB superstring theory as its classical limit, as Type IIB supergravity (ignoring the stringy and quantum effects). Recall that in Type IIB string theory, the 10-dimensional Newton constant is given by

$$16\pi G_N = (2\pi)^7 g_s^2 l_s^8. \tag{1.7}$$

Hence, for Type IIB supergravity on $AdS_5 \times S^5$ to be a valid truncation, we need the background curvature to be not only smaller than the inverse string length l_s^{-1} in order to ignore the stringy interactions (no stringy effects), but also smaller than the 10-dimensional Plank mass to ignore the higher-derivative corrections from the metric fluctuation (no quantum effects),

$$\frac{R}{l_s} = (g^2 N_c)^{\frac{1}{4}} \gg 1; \qquad\qquad \frac{R^8}{G_N} = \frac{2{N_c}^2}{\pi^4} \gg 1. \tag{1.8}$$

This however corresponds to the large-N (planar), large-λ,t Hooft (strongly coupled) regime

[10] Implicitly we also need to demand that these two procedures (decoupling limit *vs.* adiabatically dialing the coupling constant) commute, as clearly elaborated in Polchinski's TASI 2010 lecture notes [33].

of the dual $\mathcal{N} = 4$ $U(N_c)$ SYM gauge theory, establishing the strong-weak nature of the duality as mentioned above.

Intense efforts have been focused on exploiting the weakly-coupled hence tractable calculations from the gravity side, to distill otherwise intractable information of the strongly coupled regime in the field theory sides. Among the initial endeavors, one sensational thrust came from the discovery of QGP at RHIC, for it is not only the first time we discover that the *Au-Au* collisions will lead to the strongly coupled plasma (QGP) that don't comply with the quasi-particle description, but also the measured viscosity-to-entropy ratio is also quite close to the holographic calculations performed on the gravity side [23]. This hallmarks the beginning of a huge research franchise of the gauge-string duality that continues to flourish into today, upon which this thesis is built.

1.4 A Step Closer Toward Phenomenology: Quenched Matter Contents in the Fundamental Representation vs. Probe Brane Setup

It is useful here to introduce the two different schools of holographic model building towards phenomenology applications. We have discussed so far the original AdS/CFT correspondence as embedded within the superstring theory, hence its validity is demonstrated quite suggestively, if not convincingly, through the open- *vs.* closed-string description. Any similar endeavor is referred as the top-down model in the literature, as we begin from a UV-complete superstring description and, through the Maldacena limit, only later unearthing the dual pair of field theory/gravity. Contrarily, one might proceed in the reverse direction, in which one starts instead in the low-energy limit from gravity side, including all possible QG-Lagrangian terms (and bulk field contents) constrained by some symmetries one postulates to be relevant phenomenologically, performs the gravitational calculations, and only declares it later being dual to a putative, unspecified[11] strongly coupled system. Such an endeavor is referred as the bottom-up model in the literature. Apparently, in this latter direction, the exact connection between the field theory side and the string/gravity side is lost, and one can rightfully worry about the issues of UV-completion in both sides, or the

[11] One might also argue that, given the dual theory will necessary share the same global symmetries, in principle the EFT framework will select out a few, if not single out only one, from all possible field theory realizations.

associated inconsistency (even relevancy) of the effective gravity descriptions we start with. Still one might argue that this bottom-up approach nonetheless is in line with the EFT viewpoint, and is useful to exhaust all possible strongly coupled phases (in terms of all possible IR gravity solutions) that can potentially be realized through dualities, an extended notion of universality as realized through duality.

In this work, except for part of Chapter 2[12], we will be mostly working with the top-down models for phenomenology applications. However, phenomenologically speaking, one conspicuous absence in the original proposed AdS/CFT correspondence is that it only concerns field contents in the adjoint representation. Given the phenomenological interests to model matter contents in the fundamental representation, *ie.* quarks in the standard model[13], it is consequently imperative to understand how to incorporate those fundamental-representation fields into the duality framework that we have discussed thus far.

As with the top-down approach for the original AdS/CFT correspondence, the lines of reasoning also begin with the Dq-brane setting. Nevertheless, it is helpful first to digress on the special properties of D3-brane. Among all black q-brane solutions in the Type IIB supergravity, it is only with $q = 3$ that the dilaton field is a constant on the background, with the stress energy nowhere exceeding the Plank masses, hence admitting itself a consistent classical supergravity description, *ie.* without the need to resort to stringy excitations for resolving any singularities. Therefore it is usual to start with the stack of coincidental N_c D3-branes. To introduce the fundamental matters content, we can proceed by inserting an extra stack of coincidental[14] N_f number of probe Dp-branes, intersecting the given

---

[12] Notice that, even though the discussion of Chapter 2 is expressed in terms of arbitrary dimensions and an arbitrary ratio between the radius of AdS and the radius of internal space, we will eventually restrict to the D3/D5 probe system, a *bona fide* top-down model.

[13] It is also possible to model electrons/nuclei in condensed matter physics/atomic physics using probe branes. However, the logic is different: In principle, to identify the global $U(1)$ symmetry associated with charge conservation, we should use the corresponding part of the global symmetry in the gravity side, *ex.* the internal isometry dual to the R symmetry. Alternatively, it is convenient to model the "electrons" by the dual objects charged with the probe-$U(1)_B$ associated with the probe branes, and model the "phonon bath" as the probe-$U(1)_B$-neutral gluons from the $\mathcal{N} = 4$ $U(N_c)$ SYM. At large N limit, this setup hence provides a toy model for the electrons, and the lattice served as the heat bath.

[14] We can also consider splitting some m-number Dp-branes away from the main stack, leaving some coincidental $(N_f - m)$ Dp-branes behind. After taking the Maldacena limit, instead of resulting in a dual field theory with global $U(N_f)$ symmetry group as mentioned in the main text, this will lead to the

stack of N_c D3-branes, with $3 < p$ and $1 \ll N_f \ll N_c$. The open-string description of this system contains extra excitations from D3-Dp open-strings and Dp-Dp open-strings, transforming respectively under the D3- and Dp-brane worldvolume local gauge transformations as $U(N_c) \times U(N_g)$ and $U(N_f) \times U(N_f)$. After the Maldacena limit, the probe Dp-brane $U(N_f)$ worldvolume gauge coupling constant is divergent due to the $3 < p$ condition, hence "freezing out" the probe Dp-worldvolume $U(N_f)$ gauge field[15]. One is only left with the D3-Dp open-string excitations now transforming as the fundamental representation of the local gauge group $U(N_c)$ from the D3-branes, and the fundamental representation of the global symmetry group $U(N_f)$ from the previously probe Dp-branes. On the closed-string description, due to the $1 \ll N_f \ll N_c$ condition, the stress-energy of the probe Dp-branes is large enough, $S_{\mathrm{D}p} \propto \mathcal{O}(N_c N_f)$, to admit the semi-classical supergravity approximation, but is still small enough compared to the contribution from the D3-branes, $S_{\mathrm{D3}} \propto \mathcal{O}(N_c^2)$, and hence itself can be safely neglected if we only want to determine the leading part of background metric in the expansion of $\frac{N_f}{N_c}$. With this limit, $\frac{N_f}{N_c} \to 0$, referred to as the probe brane limit in the literature, we are hence left with 1) the D3-brane background of $AdS_5 \times S^5$ and N_c-unit RR 5-form flux, 2) extra probe Dp-brane worldvolume embedding fields and probe Dp-brane worldvolume gauge fields constrained by the Dirac-Born-Infeld

---

breaking of the global symmetry group, down to

$$\underbrace{U(1) \times \cdots \times U(1)}_{m} \times U(N_f - m).$$

[15] One may consider the case of $p = 3$, but since this $U(N_f)$ gauge group will not be frozen out, this will instead lead to a local $U(N_f) \times U(N_c)$ group, with the extra field content transforming in the bi-fundamental representation. The same conclusion can be reached if one still recall the splitting-off scenario as mentioned in footnote 14.

(DBI) action[16].

The above-mentioned probe brane systems [35, 36, 37] hence provide us the controlled method to model the phenomenology of strongly coupled systems with fundamental matter content, *ie.* in the quenched approximation of the field theory side, providing models for various interesting strongly coupled phenomena, ranging from the quark-gluon plasma [38, 39], unitary Fermi gas [40, 41], to high-T_c superconductor [42, 43].

1.5 Dictionary of the Gauge-String Duality

We collect here some relevant prescriptions of the duality dictionary that are used in later chapters. Given the sole purpose of understanding strongly coupled many-body systems, we mostly present the strong-weak map of the duality that associates the strongly coupled field theory to gravity. This exact (quantum-)equivalence is schematically written as:

$$Z_{\text{gauge}|_\Sigma}[\phi] = Z_{\text{string}}[\Phi|_\Sigma = \phi]. \tag{1.11}$$

However, to make this equation well-defined, we need first to specify various objects between the both sides of the equality sign. For more information, one should consult various great reviews and textbooks [23, 24].

- First, associated with each gauge-invariant local operator in the field theory side, there is an associated bulk field on the gravity side. Further more, given the global symmetries between two different descriptions are matched (as a prerequisite for the duality to hold), the associated Nöther current of the gauge theory is dual to the background gauge fields on the gravity sides.

---

[16] More precisely, for a single Dp-branes with constant worldvolume gauge strength $F_{\mu\nu}$ and worldvolume embedding $\partial_\mu\phi$, the higher oder α'-corrections can be resummed into the so-called Abelian DBI action as

$$S_{DBI} = -T_p \int d\, x^{p+1} e^{-\Phi} \sqrt{-\det\left(g_{\mu\nu} + 2\pi\alpha' F_{\mu\nu}\right)}, \tag{1.9}$$

with

$$T_p \equiv \frac{1}{(2\pi)^p g_s (l_s)^{p+1}} \tag{1.10}$$

being the Dp-brane tension, $\alpha' \equiv l_s^2$, l_s being the string length. However, in the case of coincidental branes, the non-Abelian version of the above DBI action is currently only known up to the fourth order of α' correction [34].

For instance, the global superconformal symmetry group associated with $\mathcal{N}=4$ $U(N_c)$ SYM gauge theory is realized as the isometry group of the background $AdS_5 \times S^5$ metric. Notice that even though this isometry group is a subgroup of metric transformations, its action nonetheless changes the boundary data (the explicit form of the boundary metric), therefore it is of the type of large gauge transformations, and hence it should be properly identified as the global symmetry group, according the standard quantization procedure. This leads to the prescription that the global $U(1)$ symmetric current operator J_μ in field theory is dual a $U(1)$ local gauge bulk field A_μ in gravity, and the stress-energy tensor operator $T_{\mu\nu}$ is dual to the background metric field $g_{\mu\nu}$.

In fact, in the $O(N)$-vector model/Higher Spin Gauge Theory (HSGT) conjecture, this prescription completely exhausts the operator spectrum of the $O(N)$-vector model, as every spin-s currents in the $O(N)$-vector model is dual to one Vasiliev spin-s gauge fields on AdS_3 background. In this sense, this dual pair constitutes the minimal backbone of the gauge-string duality, as reviewed by Gaberdiel and Gopakumar [44].

- Second, given one field-theory gauge-invariant local operator $\mathcal{O}_{\alpha_i\cdots\alpha_l}(x^\mu)$ dual to the associated gravity bulk field $\Phi^{\alpha_i\cdots\alpha_l}(x^\mu,z)$ with z being the radial variable chosen such that the boundary is at $z=0$[17], the generator $\phi^{\alpha_i\cdots\alpha_l}(x^\mu)$ coupled to $\mathcal{O}_{\alpha_i\cdots\alpha_l}(x^\mu)$ is dual to the rescaled boundary profile of the bulk field $\Phi^{\alpha_i\cdots\alpha_l}(x^\mu,z)$:

$$\phi^{\alpha_i\cdots\alpha_l}(x^\mu) \propto \lim_{z\to 0} \Phi^{\alpha_i\cdots\alpha_l}(x^\mu,z). \tag{1.13}$$

The intuitive picture associated with this prescription is that, given the generating functional can be regarded as the deformation of the original field theory, the dual counterpart in the gravity side must correspond to deform gravity by some non-normalizable modes, or sourced by the boundary conditions, mentioned above.

---

[17] Typically, the gravity side will be described with an asymptotic AdS ($aAdS$) background,

$$ds^2_{aAdS} \xrightarrow{z\to 0} \frac{R^2_{AdS}}{z^2}\left(dz^2 + g^{(B)}_{\mu\nu}dx^\mu dx^\nu\right) + \ldots, \tag{1.12}$$

with x^μ being the field theory direction, $g^{(B)}_{\mu\nu}$ being the boundary metric, R_{AdS} being the asymptotic AdS radius and z being the radial direction chosen such that the boundary is located at $z=0$.

For instance, for a scalar operator $\mathcal{O}(x^\mu)$ in a d-dimensional CFT, the corresponding free scalar field $\Phi(x^\mu, z)$ in the $(d+1)$-dimensional bulk gravity will admit the following expression close to the boundary $z = 0$,

$$\Phi(x^\mu, z) \xrightarrow{z\to 0} a(x^\mu) z^{d-\Delta_\mathcal{O}} + b(x^\mu) z^{\Delta_\mathcal{O}} + \ldots, \tag{1.14}$$

with $\Delta_\mathcal{O}$ being the scaling dimension of operator $\mathcal{O}(x^\mu)$, $a(x^\mu)$ being the leading term of the associated non-normalizable mode, and $b(x^\mu)$ being of the subleading, usually normalizable mode (See also the third part in the next paragraph). Therefore, the prescription is to identify $\phi(x^\mu)$ as $a(x^\mu)$, or

$$\phi(x^\mu) = \lim_{z\to 0} \frac{\Phi^{\alpha_i \ldots \alpha_l}(x^\mu, z)}{z^{d-\Delta_\mathcal{O}}}. \tag{1.15}$$

One can also check that the scaling symmetry of $\int d^d x \phi(x^\mu)\mathcal{O}(x^\mu)$ is now manifestly realized. Similarly [23, 24], for the conserved $U(1)$ current $J_\mu(x^\mu)$, the generator $a_\mu(x^\mu)$ is given as

$$A_\mu(x^\mu, z) \xrightarrow{z\to 0} a_\mu(x^\mu) + b_\mu(x^\mu) z^{d-2} + \ldots, \tag{1.16}$$

and for the conserved stress-energy tensor $T_{\mu\nu}(x^\mu)$, the generator $h_{\mu\nu}(x^\mu)$ is given as

$$g_{\mu\nu}(x^\mu, z) \xrightarrow{z\to 0} \frac{R^2}{z^2} \left(\eta_{\mu\nu} + h_{\mu\nu}(x^\mu)\right) + \ldots. \tag{1.17}$$

- Third[18], there is an isomorphism between two different Hilbert spaces.

  The Hilbert space associated with the gravity side is constructed through usual procedure of canonical quantization, *ie.* through the mode expansions of solutions for the linearized bulk equations of motion (EOMs)[19], together with some prescribed

[18] One might think that this third point should really be promoted as the first point. We here will like to point out the role played by the operators, in the non-perturbative formulation of field theory, is more fundamental than the role played by the states. Similar notions have already been encountered with spontaneous symmetry breaking in the Lagrangian formulation of QFTs. Also in algebraic quantum field theory (AQFT) formulation [45], the algebra of operators is constructed first, only later the states are realized as the special maps on the operator algebra that comply with the AQFT axioms.

[19] As the familiar cases of building up the asymptotic Fock space for QFTs on flat spacetime, the condition of linearized EOMs is required to introduce an inner product on the space of mode functions, and this product needs be linear in order to be identified as the product in the associated Hilbert space after quantization.

boundary condition, such as regularity in the bulk for zero-temperature background or in-falling at the horizon for high-temperature background. Typically, there will be two independent solutions, and due to the prescribed boundary condition, one can uniquely determine one in terms of the other. The prescribed boundary condition, together with the linearized bulk EOMs, will also single out the notion of linear inner product in field space, which typically renders one mode as normalizable, and the other as non-normalizable[20], hence facilitating the identification the former as one admissible ray, *ie. bona fide* state in the Hilbert space.

In the top-down models, explicit examples of this prescription include: 1) the vacuum state of the $\mathcal{N}=4$ $U(N_C)$ SYM gauge theory is dual to the background metric of $AdS_5\times S^5$ and the background N_c-unit of RR 5-form flux for Type IIB superstring theory, as we already seen above; 2) the thermal state at temperature T of the $\mathcal{N}=4$ $U(N_C)$ SYM gauge theory is dual to the background metric of the following form:

$$ds^2=\frac{R^2}{z^2}\left(dz^2-f(z)dt^2+\sum_{i=1}^{3}(dx^{i^2})\right)+d\Omega_5{}^2\Big|_{f(z)\equiv 1-\frac{z^4}{z_0{}^2}}, \tag{1.18}$$

with $z_0=\frac{1}{\pi T}$. Conversely, for each the normalized modes associated with each bulk field, *ie.* admissible ray in the canonically constructed Hilbert space in the gravity, there will also exist the corresponding state in field theory with the same quantum numbers.

- Fourth, even though the meanings of symbols in both sides of Eq. (1.11) are now completely specified, as it currently stands, the both sides of Eq. (1.11) are still divergent, and therefore we need to specify how to regularize and renormalize the both sides of Eq. (1.11). This part of the dictionary is referred in the literature as the holographic renormalization, which manages to systematically build up the covariant counterterms on the regularizing planes for the gravity side.

[20] However, there is a specific window of the associated parameters in which two choices of norms are possible, and the role of normalizable/non-normalizable modes will be flipped accordingly, leading to the notion of alternative quantization [46].

Given that the correct deployment of the holographic renormalization is crucial in extracting any information contained in Eq. (1.11), it will be a recurring theme in this work concerning the details of implementation in later chapters. Here, we will only briefly mention that, given the conformal boundary of the asymptotic AdS space, this "IR" singularity, due to the infinite volume of the AdS space, needs to be regulated by some "IR" cutoff at $z = \epsilon$. Recall that this singularity is in the z direction that holographically associated with an EFT defined at scale $E \approx \frac{1}{\epsilon}$. Therefore, the dictionary identifies the "IR" cutoff of the gravity side as $z = \epsilon$, with the UV cutoff of the field theory side as $E \approx \frac{1}{\epsilon}$. Here the quotation mark of "IR" is used to remind the readers that there is a issue of terminology. In the earlier literature, this cutoff was indeed referred to as "IR" from the bulk viewpoint. However, in the modern holography literature, we always adopt the boundary viewpoint, and refer to this regularization, $z = \epsilon$ as the UV cutoff. For detail information, see the review of Skenderis [47] and the literature within.

There are also specific prescriptions involving non-local operators in the field theory side, including 1) the vacuum expectation values of Wilson line operator in the field theory *vs.* the area of the associated string world sheet, which provides us the diagnostic tool for confinement/deconfinement transition using holography; 2) as also mentioned in Chapter 4, the entanglement entropy of an closed region in the field theory *vs.* the associated codimension-2 minimal surface in the gravity theory.

1.6 Outlines

In following, we will present the tools and results that we have accumulated in the study of how to better address and elucidate various properties of the strongly coupled systems with fundamental matter content in the quenched approximation. In Chap 2, we map out the first-order phase transitions associated with the bottom-up model describing the zero-temperature phases for the coupled phase between two two-dimensional defects stacked parallel in a four-dimensional ambient spacetime, dual to the presence of spontaneous symmetry breaking of the individual ultraviolet flavor symmetries associated with the double

heterostructure of the defect layers; In Chapter 3, we report on our discovery of a novel set of solutions of the probe brane system consisting of N_f D5-probe branes embedded in the near-horizon geometry generated by N_c D3-branes, with the D5 worldvolume $U(1)$ gauge fields turned on, holographically dual to a supersymmetric defect field theory at finite density in non-trivial vacua. In Chapter 4, we give a prescription for calculating the entanglement entropy in holographic probe brane systems by systematically taking the leading order backreaction of the probe brane into account. We validate our method by comparing to exact results in solvable toy models, and also determine the entanglement entropies for a sphere and a strip in the top-down D3/D7 and D3/D5 system; In Chapter 5, we state the conclusion of this work, and discuss promising directions for future study.

Chapter 2

MINIMAL SUBMANIFOLDS ASYMPTOTIC TO $ADS_4 \times S^2$ IN $ADS_5 \times S^5$

In this chapter, we recollect our previously published work, "Minimal Submanifolds asymptotic to $AdS_4 \times S^2$ in $AdS_5 \times S^5$" on Journal of High Energy Physics, vol.1404, p.037, 2014 [1], in which we construct the zero-temperature phase diagram for the coupled phase between two two-dimensional defects stacked parallel in a four-dimensional ambient spacetime, with different UV parameters turned on for different defects. We study the system in the quenched strong coupling limit, using holography via a probe brane approximation, as realized explicitly through the D3/D5 system. This coupled phase is holographically dual to the presence of spontaneous symmetry breaking of the individual ultraviolet flavor symmetries associated with the double heterostructure of the defect layers. We characterize this solution by its infrared geometric data, and present the numerical result showing a first-order phase transition between the asymmetrically coupled phase and the more mundane decoupled phase.

The organization of the chapter is as follows: In Section 2.1, we recapitulate the background materials and the main result as reported in [1]; In Section 2.2, we state our mathematical settings for the D7 and D5 embeddings in $AdS_5 \times S^5$ and introduce the notion of single-sheeted (also later called decoupled) phase for the rest of the work. We also discuss the fine points of calculation subtleties, associated with the construction of the asymmetric joint-sheeted (also latter called nontrivial coupled) phase; In Section 2.3, we present the obtained numerical results, showing a first-order transition between these two aforementioned phases.

2.1 Introduction: Interface Boundaries and Its Holographical Realizations

Of special relevance to this work are the various deformations associated with a probe-brane embedding submanifold. Such considerations are crucial in the construction of the Saki-

Sugimoto D4/D8 model [48], dual to the holographic QCD, and also fruitful in identifying various phases of the strongly coupled quantum field theory dual to the D3/D7 model [35].

Nevertheless, in the aforementioned D4/D8 and D3/D7 systems, the probe-brane embedding submanifold actually spans the whole four-dimensional external spacetime of the field theory, rendering possible only the deformation associated with the internal space. This of course is due to the feature of the physical system under study, where the quark sector roams freely together with the gluon sector. However, the idea of deformation of submanifolds, and possible interesting physical systems, are both admissible to more general consideration: Focused on the D3/D5 system, where the probe-brane system describes the defect sector confined into a two-dimensional plane, a nontrivial deformation of the submanifold for both the external and internal embedding is possible. In fact, by stacking two such defects parallel, we will show that, even when the two defect contents are in general different in their UV parameters, hence holographic dual to double heterostructure, there still exists an asymmetrically connected submanifold solution for the probe brane system. This configuration is dual to a coupled phase in the field theory side. We also will find that such an asymmetric configurations thermodynamically favorable upon some mild detuning of UV data, and there is a first-order transition from this asymmetrically coupled phases to the more mundane decoupled phase, with the increase of the difference of their UV parameters.

2.2 Methods: Minimal Submanifolds, the Two Completing Phases Thereof, and Numerical Considerations

We follow the notion used by Graham and Karch [49] for setting up our convention: They consider submanifolds asymptotic to $AdS_{k+1} \times S^l$ inside $AdS_{n+1} \times S^m$. Specialized to the D3/D5 embedding, $k = 3, l = 2, n = 4, m = 5$, this probe brane system is holographic dual to two localized defects [35, 37], with quark content of massive $\mathcal{N} = 2$ N_f-favor hypermultiplets in the fundamental representation, inserted into the background of $\mathcal{N} = 4$ $U(N_c)$ super-Yang-Mills gauge field theory, in the $N_c \gg 1$, large 't Hooft coupling limit. The two defects are separated by Δx in the common transverse direction, and each sector is characterized by its own quark mass m_L or m_R in the UV Lagrangian. We will construct

the phase diagram by tuning the dimensionless ratios, $m_L\Delta x$ and $m_R\Delta x$.

2.2.1 Submanifold Extension: mathematical settings

The mathematical setting of this article is as the following: Considering the background spacetime being a product manifold $X \times K$, where X is a $n+1$ dimensional asymptotically hyperbolic manifold with n dimensional boundary thereof, $M \equiv \partial X$, and K is a m dimensional compact manifold. The metric of $X \times K$ is parametrized using the standard Fefferman-Graham form [50]:

$$g = g_+ + g_K = \frac{dr^2 + \bar{g}_r}{r^2} + g_K, \tag{2.1}$$

with boundary M located at $r_{min} = 0$, hereafter referred as the UV end. The minimal submanifold is denoted as $Z \subset X \times K$, with boundary $\partial Z = N \times S \subset M \times K$. We can parametrize M as $(x^\alpha, u^{\alpha'})$, K as $(s^A, t^{A'})$, such that: 1) The boundary of the submanifold $N \times S$ is given by $u^{\alpha'} \to 0$, $t^{A'} \to 0$, and 2) t and u variables are "orthogonal" to the boundary, as in the following sense:

$$\bar{g}_{\alpha,\alpha'}|_{r=0,u=0} = g_{AA'}|_{t=0} = 0. \tag{2.2}$$

In this article, we focus on submanifolds asymptotic to $AdS_{k+1} \times S^l$, embedding into $AdS_{n+1} \times S^m$. We will choose to embed S^l into S^m as follows:

$$ds^2_{S^m} = d\theta^2 + \cos^2\theta d\Omega_l^2 + \sin^2\theta d\Omega^2_{m-l-1}, \tag{2.3}$$

with S^l sitting at the equator parametrized by the θ embedding function. This ansatz corresponds to the simplest symmetry-breaking pattern associated with the dual defect field theory.

Given the above parametrization, let us first consider the single-sheeted (later also called decoupled) phase of the minimal submanifold. In this phase, the minimal submanifold is not only asymptotic to $AdS_{k+1} \times S^l$, but when it extends into the bulk, the only change is the internal sphere radius, controlled by the θ embedding function, being endowed with nontrivial radial dependence, $\theta = \theta(r)$. All external-space embeddings are constant, hence no "bending" of the probe external location occurs along the radial direction. In fact,

notice that radial dependence is actually the most generally allowed dependence if we insist on preserving the defect-translational invariance, as well as S^l and S^{m-l-1} isometries for the dual field theory. With the standard Poincaré patch for AdS_{n+1} and static gauge for AdS_{l+1}, the area of the submanifold is then given by:

$$S = \int dr \frac{\cos^l \theta}{r^{k+1}} \sqrt{1 + \alpha^2 r^2 (\theta')^2}, \tag{2.4}$$

where α is a generalization introduced to account for the possible difference between the curvature radii of internal compact space S^m and the external AdS_{k+1} space, $\alpha \equiv (R_{S^m}/R_{AdS_{k+1}})$. $\alpha = 1$ in $AdS_5 \times S^5$, the standard near-throat limit of supergravity background generated by from the D3 brane. Given that the D3/D5 system is our primary concern, hereafter we commit ourselves to the $\alpha = 1$ case. Also we have set $R_{AdS_{k+1}}$ to 1. The usual variational method yields the equation of motion for $\theta(r)$ as:

$$\theta'' = -l \left(\frac{1}{r^2} + (\theta')^2 \right) \tan\theta + (\frac{-1+k}{r})\theta' + kr(\theta')^3. \tag{2.5}$$

Let's first consider the special case of the D3/D7 system, where the D7 probe brane is asymptotic to $AdS_5 \times S^3$ ($k = 4, l = 3$): This submanifold is completely filling the external space of the background spacetime, and we can easily check that we then have an one-parameter family of embeddings, $\theta = \arcsin(mr)$, with m being the free parameter. θ is the so-called slipping mode in the literature. The same solution also holds for the D3/D5 system, with the probe brane embedding submanifold asymptotic to $AdS_4 \times S^2$ ($k = 3, l = 2$). Such a simple analytical result is connected with the supersymmetry of the probe brane system [51]. In more general systems, however, one can only observe that θ being zero is still a solution, which extends into the one-parameter family of solutions by turning on the slipping mode with the initial slope, $\theta(r) = mr + \mathcal{O}(r^2)$. But one will need to numerically integrate out the equation to complete the profile.

However, we are naturally more interested in configurations with the external embedding being nontrivial, specifically the joint-sheeted configuration, corresponding to two defect stacked parallel to each other, with the submanifolds bending towards each other and eventually smoothly joined in the radial direction. An example of this connected configuration is the Wilson line used by Maldacena [52] to compute the quark-antiquark force: Near the

boundary the submanifold is asymptotic to AdS_2 times a point. However, deep inside the bulk, the submanifold is connected into a U-shaped configuration. Therefore, in this article, we parametrize such a connected submanifold as being the union of two different branches, $\partial Z = (N_1 \times S_1) \bigcup (N_2 \times S_2)$, with each branch chosen to be $N_i \times S_i = R^k \times S^l$. As mentioned before, to preserve the dual field theory symmetries associated with the symmetries of both the defect space and the transverse space, only radial dependence is admissible for the embedding functions. For simplicity, instead of the simple internal global symmetry breaking pattern chosen by Eq.(2.3), we will also restrict ourselves by only turning on one nontrivial external embedding function, hereafter named $x(r)$. Still working in the standard Poincaré patch for AdS_{n+1} and static gauge for AdS_{l+1}, the area of the submanifold is modified as:

$$S = \int dr \frac{cos^l\theta}{r^{k+1}} \sqrt{1 + (x')^2 + r^2(\theta')^2}, \tag{2.6}$$

with the equations of motion given by:

$$\begin{aligned} x'' =& \frac{(1+k)}{r}(x')^3 + x'\left(\frac{1+k}{r} + kr(\theta')^2\right); \\ \theta'' =& -l\left(\frac{1+(x')^2}{r^2} + (\theta')^2\right)\tan\theta + \frac{-1+k+(1+k)(x')^2}{r}\theta' + kr(\theta')^3. \end{aligned} \tag{2.7}$$

However, unlike the previous single-sheeted phase, these equations admit no analytical solution at least to us, and hence we are forced to resort to numerical methods for computing the profile.

2.2.2 The Regularity Constraint and the Cascaded Integration Scheme

To solve the embedding equations Eq.(2.7), the boundary conditions, required to generate the joint-sheeted configurations, are given by requiring the connection of the two branches inside the bulk space being smooth. This however renders $x'(r)\big|_{r\to r_{max}}$ divergent and further denies us control over the boundary specification at r_{max}, the turning point of the joint-sheet submanifold. Nevertheless, this seeming difficulty can be resolved by a closer inspection of the regularity requirement: Notice that the Lagrangian density is cyclic in the x-parameter, hence conserving the conjugated momentum thereof,

$$\Pi_x \equiv \frac{\partial L}{\partial x'} = \frac{cos^l\theta}{r^{k+1}} \frac{x'}{\sqrt{1 + (x')^2 + r^2(\theta')^2}}. \tag{2.8}$$

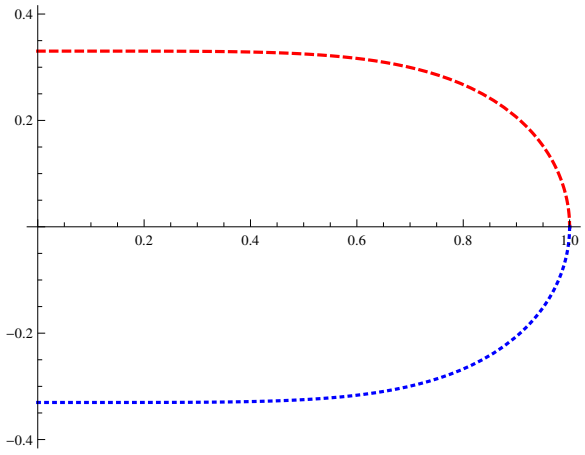

Figure 2.1: $x(r)_{symmetric}$: A typical result for a symmetrically connected configuration. Within the r-parametrization, this coupled configuration is expressed by two separate but identical branches joining smoothly at the turning point r_{max}, normalized to 1 in above.

Therefore, we can express x' in term of this integral of motion Π_x,

$$x' = \pm \sqrt{\frac{1 + r^2(\theta')^2}{\left(\frac{cos^l\theta}{\Pi_x r^{k+1}}\right)^2 - 1}}. \tag{2.9}$$

The regularity requirement therefore translates into the following two scenarios: First, we have the denominator equal to zero, providing a condition relating all the parameters at the IR end:

$$\left[\left(\frac{cos^l\theta}{\Pi_x r^{k+1}}\right)^2 - 1\right] \xrightarrow{r\to r_{max}} 0; \tag{2.10}$$

Second, we have the numerator equal to infinity, signaling at the IR end sitting not only a divergent $x'(r_{max})$ but also a divergent $\theta'(r_{max})$ as well:

$$\frac{d\theta}{dr} \xrightarrow{r\to r_{max}} \infty. \tag{2.11}$$

One may expect the first scenario to be more relevant, given the smoother behavior of $\theta(r)\big|_{r\to r_{max}}$. But further analysis, by expanding the submanifold in power series given the regular behavior of $\theta(r)$ around r_{max}, reveals that the first scenario is actually too restrictive. It constrains the two branches of the submanifold to be exactly the same, ending with only

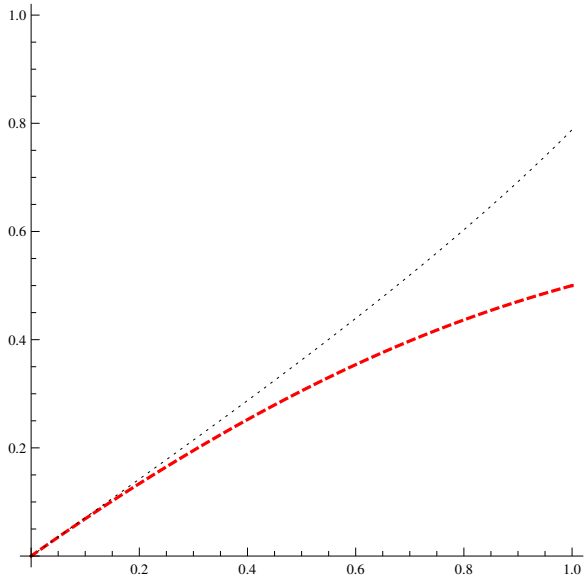

Figure 2.2: $\theta(r)_{symmetric}$: A typical result for a symmetrically connected configuration. Within the r-parametrization, this coupled configuration is expressed by two separate but identical branches joining smoothly at the turning point r_{max}, normalized to 1 in above. In this figure, the dotted line stands for the asymptotically decoupled configuration with the same UV parameter, the asymptotic mass term $m_{asymptotics} \equiv \theta'(r)\big|_{r\to 0}$. Notice we use the translational invariance to set $x(r_{max}) = 0$.

symmetric joint-sheet configurations. Therefore, to include the most general, asymmetric joint-sheeted configuration, the second scenario and hence singular behavior of $\theta(r)$ around r_{max} will need to be considered.

To numerically generate the solution given by the second scenario for the boundary conditions, we adopt the following cascaded integration scheme: First, around $r \sim r_{max}$, we choose to parametrize the solution in terms of the x-variable, with the equations of motion given by:

$$r'' = -\frac{1+k}{r}(1+(r')^2) - kr(\theta')^2; \tag{2.12}$$

$$\theta'' = -l\left(\frac{1+(r')^2}{r^2} + (\theta')^2\right)\tan\theta - 2\frac{r'}{r}\theta'. \tag{2.13}$$

Choosing the turning point to be at $x_0 = 0$, the solution is uniquely determined by the

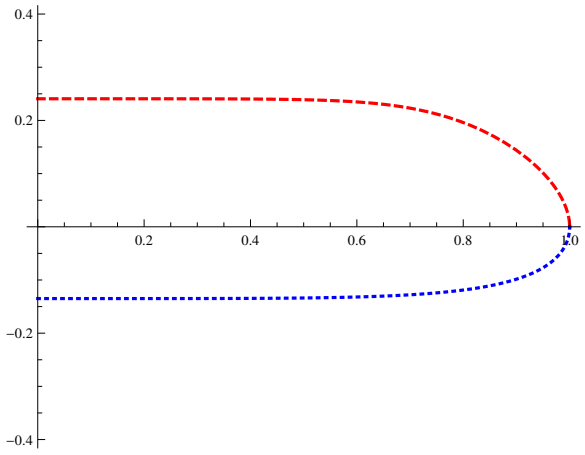

Figure 2.3: $x(r)_{asymmetric}$: A typical result for an asymmetrically connected configuration. Within the r-parametrization, this coupled configuration is expressed by two separate and different branches joining smoothly at turning point r_{max}, normalized to 1 in above.

"IR" data: $\{r(x_0) \equiv 1, r'(x_0) \equiv 0, \theta(x_0), \theta'(x_0)\}$, located at r_{max}. Therefore, the entire solution family are indeed generated by 4 parameters: $\{\theta(x_0), \theta'(x_0), r(x_0), x_0\}$, with the later 2 generated from dilatation and translation symmetry. Given the equations are regular in terms of the x-variable, we perform the numerical integration to a predetermined intermediate point away from the boundary. However, given the equations is singular in terms of x-variable at the boundary, to approach the boundary with more numerical stability, we will then switch over to the r-parametrization before carrying out the integration to the boundary. With such a cascaded scheme, we can numerically find the most general, asymmetric connected configuration.

2.2.3 Extraction Scheme

The great virtue of the probe brane approximation is that various physical quantities of interest can be obtained without re-solving the Einstein equation with the probe source, as long as those quantities can be calculated using the free energy and thermodynamical relations, as already explained in [53]. Therefore, to determine the phase diagram, we can follow this tenet and simply compute the free energy using the on-shell action for the given config-

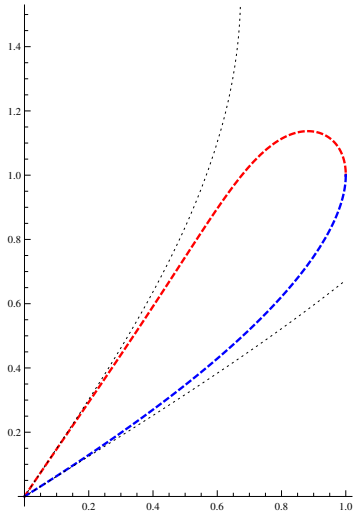

Figure 2.4: $\theta(r)_{asymmetric}$: A typical result for an asymmetrically connected configuration. Within the r-parametrization, this coupled configuration is expressed by two separate and different branches joining smoothly at turning point r_{max}, normalized to 1 in above. In this figure, the dotted lines stand for the corresponding asymptotically decoupled configuration for each branch, with different mass terms on the different side of the lobe. We can generate such graph within the x-parametrization from the IR end, and cascade with the r-parametrization when approaching the UV end. Notice we use the translational invariance to set $x(r_{max}) = 0$.

uration, and determine which phase, single-sheeted (also called decoupled) or joint-sheeted (also called coupled), is thermodynamically favorable. However, the boundary divergence of AdS space renders the first step rather laborious: the canonical approach is to deploy the holographic renormalization [54], which carefully reconstructs the diffeomorphism-invariant counterterms by examining the divergent structure associated with the tentative cut-off plane, dual of the UV regulator for field theories. However, in this study, given that we eventually only focus on the difference of free energies between the decoupled and coupled configurations, we will adopt the following extraction scheme (also known as background subtraction): given any coupled configuration, we first construct the dual disconnected configuration with the same UV parameter $m_{asymptotic}$. Then the difference of these two

configurations is, by construction, vanishing near the boundary, since all coupled configurations are asymptotic to the decoupled solution in the UV region (See Fig.2.2-2.4).

The rationale behind our extraction scheme is that the to-be-constructed holographic counterterms can only depend on the UV behaviors but not IR physics, which is already present in the decoupled configuration once the only relevant information, m_L or m_R is extracted. This scheme is also more in tune with the pre-Wilsonian renormalization philosophy, "sweeping under the rug", that no divergence should be present if every physical prediction is expressed with physical quantities.

In practice, given we can only work with the numerically generated configuration, there is a potential caveat associated with such an extraction scheme: the UV parameter $m_{L/R}$ is located at the singular point of the equations of motion, and we only extract this information numerically up to a small cut-off distance due to the inevitable numerical instability. Such a seemingly simple numerical recipe can be subject to more elaborate modification: One can construct the analytic solution expanded around the singular point, and extract the parameters by fitting at a point away from boundary, with now more numerical control. However, given the phase transition we find is of first order in nature, and in the precision we are working on, the difference thus introduced is found to be numerically negligible with no qualitative change of the conclusion.

2.3 Main Results: Numerical Phase Diagrams and the Associated First-Order Phase Transistions

2.3.1 Symmetric Coupled Phase

We first restrict to the symmetric connected configurations only. Fig.2.6 shows the on-shell area difference, which is also the free energy difference, between the symmetric coupled and decoupled configurations as a function of the normalized mass term $\xi_{normalized}$:

$$\xi_{normalized} = m\Delta x, \tag{2.14}$$

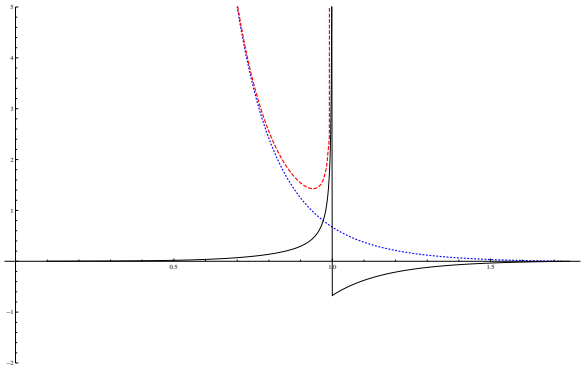

Figure 2.5: A typical extraction result of comparing the Lagrangian (submanifold volume density) with r, the AdS radial direction: Red(dashed) line, a typical coupled configuration; Blue(dotted) line, the dual decoupled configuration; Black(thin) line, the difference between the previous two, with the signed area being the free energy difference. One can observe the divergence term is indeed subtracted out when approaching the boundary, and the difference is only due to the back reaction inside the bulk. Notice in this specific case the decoupled configuration can extend deeper into the bulk even after the coupled counterpart already terminates ($r_{max} = 1$ by normalization). The reverse situation also is possible, where the decoupled surface can terminate before the connected one.

with

$$\begin{aligned} m &= \theta'(r_{min}) \\ \Delta x &= x(r_{min})\big|_{upper-branch} - x(r_{min})\big|_{lower-branch}. \end{aligned} \tag{2.15}$$

For every value of $\xi_{normalized}$ we find two coupled solutions. At very low $\xi_{normalized}$, one of the symmetric coupled configuration is the thermodynamically favored phase, compared with its decoupled counterpart(with negative free energy difference); as $\xi_{normalized}$ increases, the area difference begins to shrink, and finally a first order phase transition is reached when $\xi_{normalized}$ reach the value of 0.165, after which the decoupled dual becomes more favorable ones; however, as $\xi_{normalized}$ keeps increasing and eventually above 0.315, the coupled configuration disappears entirely, and only the decoupled phase exists as the only allowed solution for the minimal submanifold.

Figure 2.6: Indication of the first order phase transition of symmetrically coupled submanifold as $\xi_{normalized}$ changes. The vertical axis shows the difference of surface area between the coupled configuration and its decoupled counterpart; the horizontal axis is the characteristic label of the connected surface defined in Eq.(2.14).

2.3.2 Asymmetric Coupled Phase

Using the cascade evolution scheme, we can also compute the phase diagram for the asymmetric connected configuration. Fig. 2.7 and Fig. 2.8 show the phase diagram of the first order phase transition for the minimal submanifold between the asymmetric coupled and decoupled configurations as a function of two physical parameters:

$$\xi_i = m_i(\Delta x), i \in \{L, R\}; \tag{2.16}$$

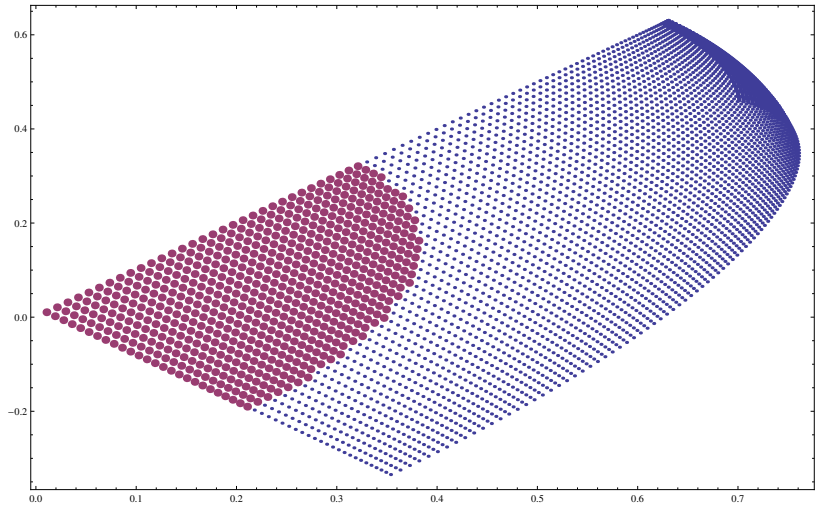

Figure 2.7: Phase Diagram for Asymmetrically Coupled Configuration: Indication of the first order phase transition of asymmetrically coupled submanifold as ξ_L and ξ_R are varied. Given the solution is enumerated with the IR data, $\theta(r_{max})$ and $\theta'(r_{max})$, we perform the numerical scan by constructing the constant $\theta'(r_{max})$-curve and slowly filling up the entire phase space, where in the red (heavy-shaded) region the coupled phase dominates. Notice the upper corner is present due to our scanning procedure: The solution is scanned by varying the IR data, but the phase diagram is labeled by the dimensionless parameters back-constructed from UV properties of the obtained solution. This leads to the same upper lope as in Fig.2.6.

with

$$\begin{aligned} m_i &= \theta_i'(r_{min}) \\ \Delta x_i &= \left|x_i(r_{min})\right|, i \in \{L, R\}, \end{aligned} \tag{2.17}$$

where we use L and R to denote the different branch under study. Notice that due to the reflection symmetry of the parameter space along the axes of both $\xi_L = \xi_R$ and $\xi_L = -\xi_R$, we only need to scan the portion of Fig. 2.7. In Fig.2.8, the partial scanning of the free energy density difference is also shown, which explicitly demonstrates that the phase transition is also of the first-order.

2.4 Conclusion

In this chapter we summarized our previous work on investigating the submanifolds asymptotic to $AdS_4 \times S^2$ embedded into $AdS_5 \times S^5$. We restrict to the largest unbroken residual symmetry. We find the asymmetric joint-sheeted configuration, with both external embedding and internal embedding radially deformed. These are dual to the coupled phase between two two-dimensional defects stacked parallel, with different UV parameters. While similar phases have been studied previously in the probe brane systems, what is novel about our work is that the asymmetric probe brane system is holographic dual to the double heterostructure in condensed matter systems, with different UV data in the two layers. The asymmetrically coupled phase is holographic dual to the spontaneous symmetry breaking of the original decoupled ultraviolet $U(N_f)_L \times U(N_f)_R$ flavor symmetries, associated with flavor rotation for individual defect content, into the diagonal subgroup $U(N_f)$ due to the non-vanishing condensate developed at infrared, $\langle \bar{\psi}^i_a (e^{\int A})^a{}_b \psi^{j,b} \rangle$. This order parameter has also been studied in [55] for the chiral condensate of Saki-Sugimoto model. Solutions are shown completely parametrized by the infrared geometric data, being the IR value and slope of the internal deformation, upon which the entire profile is numerically constructed by the cascading integration scheme we adopted in this paper. Aimed with the complete numerical solution, we map out the phase diagram between this asymmetrically coupled phase and the competing mundane decoupled phase, and we find that the coupled phase is dominating at zero temperature, even when the UV parameters are mildly detuned, and with large enough difference the system undergoes a first-order phase transition to the decoupled phase.

Notice that more general deformations of the submanifolds are possible, corresponding to finer symmetry breaking pattern in the dual field theory side. Such details present no challenge for profile construction using the cascading integration scheme. However the corresponding phase diagram is computationally difficult to enumerate: For example, in the cases of deforming two internal embedding functions, *ie.* $\theta = \theta(r)$ and $\psi = \psi(r)$, we find that this solution can be constructed with 4 degrees of freedom, being their IR values and slopes of the two internal coordinates. The phase diagram will be 4 dimensional, which present itself an expensive numerical barrier. Tracing out this space to locate the transition

boundary and hence its transition nature will be left for future investigation.

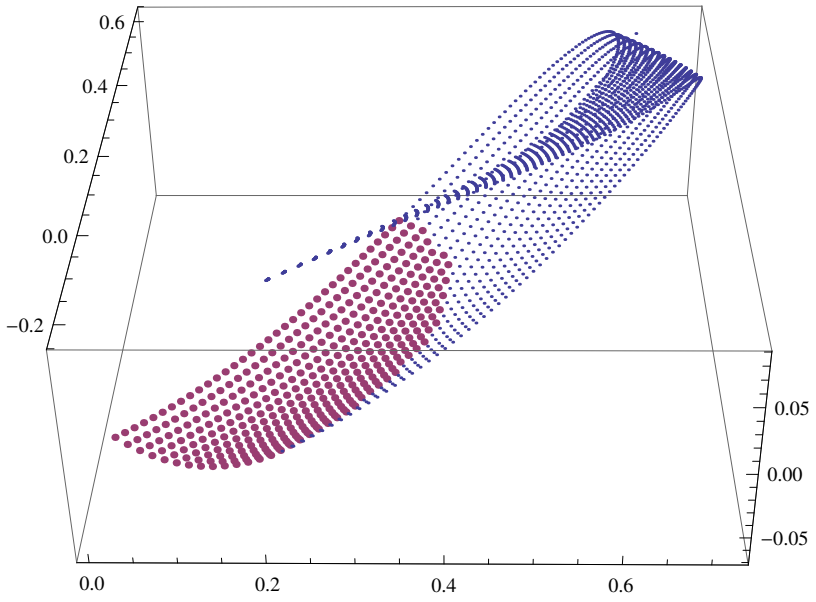

Figure 2.8: A snapshot of numerical scanning of the free energy difference with constant $\theta'(r_{max})$-curves: Indication of the first order phase transition of asymmetrically coupled submanifold as ξ_L and ξ_R are varied. Given the solution is enumerated with the IR data, $\theta(r_{max})$ and $\theta'(r_{max})$, we perform the numerical scan by constructing the constant $\theta'(r_{max})$-curve and slowly filling up the entire phase space, where in the red (heavy-shaded) region the coupled phase dominates. Notice the upper corner is present due to our scanning procedure: The solution is scanned by varying the IR data, but the phase diagram is labeled by the dimensionless parameters back-constructed from UV properties of the obtained solution. This leads to the same upper lope as in Fig.2.6.

Chapter 3

NOVEL SOLUTION IN D3/D5 WITH FINAL DENSITY

In this chapter, we recollect our previously published work, in collaboration with Prof. Andreas Karch, "The Novel Solutions of Finite-Density D3/D5 Probe Brane System and Their Implications for Stability" on Journal of High Energy Physics, vol.1210, p.060, 2014 [2], in which we discover a novel set of solutions of the probe brane system consisting of N_f D5-probe branes embedded in the near-horizon geometry generated by N_c D3-branes, with the D5 worldvolume $U(1)$ gauge fields turned on. Our system is holographically dual to a supersymmetric defect field theory at finite density in non-trivial vacua. We find that a large class of vacua turns out to satisfy a no-force condition, even with supersymmetry explicitly broken by the finite density; our solutions include configuration in which charge separates from the horizon and is instead carried by probe branes outside the horizon. The free energy is lowered in this process. Whether this corresponds to a genuine instability of the finite-density probe brane system remains to be seen.

The organization of the chapter is as follows: In Sec.3.1, we recapitulate the notion of defect conformal field theories and motivate the associated holographical model via a probe construction, *ie.* the D3/D5 probe brane system; In Section 3.2, We state the settings of our notions for D3/D5 probe brane system; In Section 3.3, we present the main result, *ie.* the novel solution that we find in the quantum liquid dual to the D3/D5 system at finite density in the probe brane approximation; In Section 3.4 we discuss the stability of this novel finite-density configuration.

3.1 Defect Conformal Field Theories and D3/D5 Probe Brane System: Review

Of special interest to this work is the probe brane system consisting of intersecting D3/D5 branes [36, 37]: The dual gauge theory picture is the flavoring of the bulk $\mathcal{N} = 4$ SYM theory by the introduction of fundamental representation matter confined on a codimension-one

defect. The localized matter consists of N_f $\mathcal{N} = 2$ supersymmetry-preserving hypermultiplets. In the weakly coupled brane system, these extra fundamental degrees of freedom are provided by the D3-D5 open strings. In the gravity side, only the gauge invariant operators including at least two flavor fields are visible; their spectrum is encoded in the fluctuations of the 5-5 fields in the bulk. The preserved supersymmetry manifests itself through a no-force condition (this can also be shown explicitly using the κ symmetry).

The Higgs phase of the probe brane system is also well-known [37, 56, 57, 58]. By turning on the probe brane worldvolume field strength, the background Ramond-Ramond 4-form potential is coupled to the probe brane action through the Wess-Zumino term. This is equivalent to separating some of the color D3 branes from the stack of N_c D3 branes hiding behind the horizon and dissolving them into fluxes inside the flavor branes carrying corresponding D3-brane charges. This has been realized by introducing probe brane worldvolume magnetic flux in the D3/D5 system, and instanton fields in the D3/D7 system. In the gauge theory picture, this splitting of color branes partially breaks the color gauge symmetry, and induces the vacuum expectation values of the quark content bounded at the defect.

In this work we are mostly interested in brane systems corresponding to the field theory at finite baryon number chemical potential. In the holographic investigation of the finite-density quantum field theories, one constructs the dual gravity solution by turning on the probe brane worldvolume electric flux to generate the non-vanishing time component of the gauge potential at the boundary. Latter is dual to non-vanishing chemical potential in the field theory through the AdS/CFT dictionary. Since the resulting field theory system retains finite entropy even at zero temperature, there is a macroscopic degeneracy associated with the vacuum state. While this degeneracy may well be just an artifact of the large N_c and large 't Hooft coupling limit underlying our construction, it may also indicate that we are expanding around the wrong vacuum and hence a potential instability under fluctuations. Perturbative stability of the D3/D7 probe brane system has been investigated by Ammon, et al. [59], where they found that in spite of all the arguments favoring instability, the D3/D7 probe brane system remains stable within the realm of perturbative fluctuations. To investigate the non-perturbative fluctuations, however, one will need to obtain the in-

formation about other possible configurations smoothly connected to the fiducial vacuum state dual to the gravity solution. One potential instability is towards disintegration of the central stack of D3 branes; probe D3 branes could separate from the bulk horizon and carry some fraction of the baryon number with them. In the D3/D7 system these probe D3 branes should dissolve themselves as instantons inside the flavor D7 brane, moving the system into the Higgs phase [56]. In order to see whether the system is stable, meta-stable or unstable towards disintegration of the central D3 brane stack, we are hence required to study the system on its Higgs branch at finite density. For the D3/D7 system, progress in this direction is hampered by the fact that one is dealing with instanton configurations. In the D3/D5 system, the Higgs branch simply corresponds to magnetic flux and is more tractable. Nevertheless, one is being faced with having to solve complicated non-linear partial differential equation derived from the Born-Infeld action.

3.2 D3/D5 Probe Brane System: Mathematical Setting

In this section we briefly state the dual gravity construction of the defect conformal field theory. The complete dictionary can be found in [37]. The intersecting D3/D5 probe brane is given by the following probe configuration in the flat 10-dimensional Minkowski spacetime:

	x^0	x^1	x^2	x^3	x^4	x^5	x^6	x^7	x^8	x^9
D3	x	x	x	x	o	o	o	o	o	o
D5	x	x	x	o	x	x	x	o	o	o

In the supergravity limit, the near-horizon metric generated by the N_c D3 color brane is given by:

$$ds^2 \equiv g_{\mu\nu}dx^\mu dx^\nu = \frac{1}{{r_6}^2}(-dt^2 + d\vec{x}^2) + \frac{1}{{r_6}^2}(d{r_6}^2 + {r_6}^2 d\Omega_5^2), \tag{3.1}$$

where r_6, the AdS radial direction, is given by:

$$r_6 = \sqrt{(x^4)^2 + (x^5)^2 + (x^6)^2 + (x^7)^2 + (x^8)^2 + (x^9)^2}. \tag{3.2}$$

There is no dilaton associated with the supergravity background generated by the D3 color branes; however, the background contains the Ramond-Ramond 5-form field strength, with

the Ramond-Ramond 4-form potential given by:

$$C^{(4)} = \frac{r^4}{R^4} dx^0 \wedge dx^1 \wedge dx^2 \wedge dx^3. \tag{3.3}$$

We are considering the probe brane limit, $N_f \ll N_c$, equivalent to ignoring the back-reaction of the D5 probe branes upon the background geometry. We also turn on the probe brane worldvolume field strength associated with the $U(1)$ factor of the $U(N_f)$ gauge group on N_f coincident D5 probe brane, anticipating the application as a dual description of a defect field theory with non-vanishing $U(1)_B$ charges. In the probe limit, the D5 probe branes simply minimize their worldvolume action in a fixed background. The action is the sum of the corresponding Dirac-Born-Infeld action describing the geometric embedding within the throat geometry and the Wess-Zumino term associated with the background Ramond-Ramond 4-form potential:

$$S_{D5}^{DBI} = -N_f T_{D5} \int d^6\xi \sqrt{-\det\left(P[g] + \tilde{F}\right)}, \tag{3.4}$$

$$S_{D5}^{WZ} = N_f T_{D5} \int P[C] \wedge \tilde{F}. \tag{3.5}$$

Using static gauge, $(\xi^0, \xi^1, \xi^2, \xi^3, \xi^4, \xi^5) \equiv (x^0, x^1, x^2, x^4, x^5, x^6)$, the bulk field content includes: the embedding function for the boundary coordinate, $x^3(\xi^i) \equiv \phi(\xi^i)$; the embedding functions for the internal bulk coordinate, $x^7(\xi^i) \equiv \eta(\xi^i)$ and $x^{8,9}(\xi^i)$; the D5 world volume field strengths, $F = B + E \wedge dt$. To maintain the translational symmetry of the boundary theory, all the dependence on the boundary coordinates will be eliminated, hence the bulk fields only depend on the internal space coordinates, $\xi^{3,4,5}$. We will be looking for the dual theory with supersymmetry preserving massive hypermultiplet. The mass corresponds to non-zero separation between D5 and D3 branes. In the weakly coupled brane setup, the open strings spanning from D5 to the D3 branes give rise to the featured massive hypermultiplets. A simple supersymmetric solution to the equations of motion is obtained by setting x_7, x_8 and x_9 to be constant [35]. We will utilize the $SO(3)$ symmetry of the internal symmetry to rotate the solution so that $x^7 = m$, $x^8 = x^9 = 0$. m is a free parameter; effectively we see that our system realizes a no-force condition. This is a manifestation of the supersymmetry preserved by this setup.

3.3 The Novel Solutions

In this section we present the main result of this paper, the novel solutions for the probe brane system with the presence of the probe brane worldvolume electric and magnetic field strengths. In the following, given that the bulk field content only depends on the 3-dimensional internal space, we will abuse notation and denote the formulae in vector notation for differential operators associated the internal coordinates.

3.3.1 Solutions with Only Non-Trivial Worldvolume Magnetic Field Strength Present

We first investigate the situation with only the world-volume magnetic fields turned on, upon which the Lagrangian densities of the D5 probe brane action can be reduced into the following forms:

$$\begin{aligned} \mathcal{L}_{D5} &= \mathcal{L}_{D5}^{DBI} + \mathcal{L}_{D5}^{WZ}, && (3.6)\\ \mathcal{L}_{D5}^{DBI} &= -\sqrt{1 + {r_6}^4(|\vec{B}|^2 + |\nabla\phi|^2) + {r_6}^8(\vec{B}\cdot\nabla\phi)^2}, && (3.7)\\ \mathcal{L}_{D5}^{WZ} &= {r_6}^4\vec{B}\cdot\nabla\phi. && (3.8) \end{aligned}$$

This complicated system of partial differential equations however admits one particular set of solutions: guided by BPS techniques, where the second-order operator is decomposed into product of first-order operators, we notice that the Lagrangian density only depends on the derivatives of boundary embedding function $\phi(\xi^i)$, hence the functional derivative of the action with respect to ϕ field gives:

$$\partial_i\left(\frac{\partial\mathcal{L}}{\partial\phi_{,i}}\right) = 0. \tag{3.9}$$

A simple ansatz for solving this equation is to require that the variation of the action with respect to the gradient of the scalar field vanish identically (and not just its divergence).

$$\frac{\partial\mathcal{L}}{\partial\phi_{,i}} = 0. \tag{3.10}$$

This ansatz can be simplified into the following relation between the magnetic fields and the boundary embedding function:

$$0 = \frac{\partial\mathcal{L}}{\partial\phi_{,i}} = \frac{-{r_6}^4\phi_{,i} - {r_6}^8(\vec{B}\cdot\nabla\phi)B_i}{\sqrt{1 + {r_6}^4(|\vec{B}|^2 + |\nabla\phi|^2) + {r_6}^8(\vec{B}\cdot\nabla\phi)^2}} + {r_6}^4B_i$$

$$\Rightarrow \vec{B} = \nabla\phi. \tag{3.11}$$

With this ansatz explicitly spelled out, it now becomes straightforward to check that the rest of equations of motion are solved: due to the symmetry between B_i and $\phi_{,i}$ in the Lagrangian density, it is easy to see that the equations of motion for gauge potentials are satisfied:

$$0 = \partial_j \left(\frac{\partial \mathcal{L}}{\partial A_{i,j}} \right) = \partial_j \left(\frac{\partial B_k}{\partial A_{i,j}} \frac{\partial \mathcal{L}}{\partial B_k} \right); \tag{3.12}$$

The equation of motion for η field (that is the x^7 coordinate) is also solved for any constant $m \equiv \eta_0$ assignment:

$$\begin{aligned} 0 = \frac{\partial \mathcal{L}}{\partial \eta} &= \frac{\partial {r_6}^4}{\partial \eta} \frac{\partial \mathcal{L}}{\partial {r_6}^4} \\ &= \frac{\partial {r_6}^4}{\partial \eta} \left(\frac{1}{2} \frac{-(|\vec{B}|^2 + |\nabla\phi|^2) - 2{r_6}^4 (\vec{B}\cdot\nabla\phi)^2}{\sqrt{1 + {r_6}^4(|\vec{B}|^2 + |\nabla\phi|^2) + {r_6}^8 (\vec{B}\cdot\nabla\phi)^2}} + \vec{B}\cdot\nabla\phi \right). \end{aligned} \tag{3.13}$$

It is easy to check that with our solution for ϕ and $\vec{B}$ the expression in parentheses vanishes identically.

Notice that the ansatz Eq.(3.11) completes the square of the DBI part of the Lagrangian density Eq.(3.7), which cancels all nontrival field dependence from the Wess-Zumino part Eq.(3.8). This leads to a constant on-shell Lagragian density irrespective of any detail of the solutions within this sector, not even the mass scale m associated with the transverse splitting between D3 and D5 branes. This is of course a signal of the preserved supersymmetry. These solutions correspond to the supersymmetry preserving Higgs branch of the dual defect field theory.

To understand the geometry of these solutions, note that we can turn on any arbitrary boundary embedding function, $\phi = \sum_i \frac{q_i}{|r_3 - r_i|}$ ($r_3 \equiv \sqrt{\xi^3 + \xi^4 + \xi^5}$), while preserving the no-force condition. The corresponding $\frac{1}{|r_3 - r_i|}$ spikes in the scalar field at the positions r_i can be interpreted as D3-branes ending on the D5 probe brane, as pointed out by Callan and Maldacena [60]. The endpoint of the D3 brane sources the magnetic worldvolume field which (through the Wess-Zumino action Eq.(3.8)) ensures that the D5 brane carries D3 brane charge and so we don't violate D3 charge conservation. Our bulk solution describes

hence an arbitrary number of half D3 branes ending on either side of the D5 branes at arbitrary positions in the 3d internal space. We can label the general solution by the positions r_i and the numbers q_i of D3 branes ending at at given r_i. The signs of the q_i indicate in which side of the D5 a given half-D3 ends. Schematically such a supersymmetric Higgs branch configuration is displayed in panel (a) of figure 3.1.

The special case of a single stack of half-D3 branes ending at the origin $\nabla \cdot B = \nabla^2 \phi = Q\delta^3(r)$ while setting $m = 0$ has been analyzed previously [36, 57, 61]. Using the spherical symmetry of the system, this can be recast as an embedding wrapping a constant S^2 inside S^5 with Q units of worldvolume magnetic flux piercing the S^2. The embedding coordinate x^3 (described by the field ϕ) now only depends on the radial coordinate. As ϕ only appears in the equations derivatively, one can simply integrate the resulting ordinary differential equation; the result is in complete agreement with our general solution. In this special case, one can even find the corresponding finite-temperature solution [61].

The single magnetic charge at the origin with non-zero mass is also a very interesting special solution, first discussed in [57]. In the weakly coupled brane picture, we have a single half-D3 brane ending on the stack of N_f D5 branes, but the whole D5/half-D3 merged brane configuration is separated from the stack of N_c color D3 branes by a distance proportional to the mass. In the holographic dual description, we have a probe brane that is not touching the horizon. The D5 brane turns into a single spike running parallel to the horizon off to infinite x_3. Waves incoming from the boundary can be supported with any frequency, so the system has no gap. This seems to be the only known example of a probe brane that supports massless fluctuations but doesn't touch the horizon. The fluctuations originally localized on the D5 can run off to spatial infinity in the transverse x_3 direction.

3.3.2 Non-Trivial Worldvolume Electric and Magnetic Field Strength

Introducing the electric field strength $\vec{E}$ on the D5 probe brane worldvolume will not modify the coupling of the background Ramond-Ramond 4-form potential from Wess-Zumino part of the action Eq.(3.8), but the DBI part becomes more complicated:

$$\mathcal{L}_{D5}^{DBI} = -\sqrt{1 - |\vec{E}|^2 + {r_6}^4(|\vec{B}|^2 + |\nabla\phi|^2 - (\vec{B}\cdot\vec{E})^2 - |\vec{E}\times\nabla\phi|^2) + {r_6}^8(\vec{B}\cdot\nabla\phi)^2}. \quad (3.14)$$

We will employ the similar reduction method as before, that is we demand that the variation of the action with respect to the gradient of the scalar field vanish identically. Solving Eq.(3.10) we find:

$$\vec{B} \ = \sqrt{1-|\vec{E}|^2}\nabla\phi + \frac{\vec{E}\cdot\nabla\phi}{\sqrt{1-|\vec{E}|^2}}\vec{E}. \tag{3.15}$$

With this relation, a tedious but straightforward algebraic exercise reveals that the full set of equations of motion is reduced into a single constraint. More explicitly, one finds that this ansatz alone not just solves the equations of motion for the ϕ field. In addition, once more the equations of motion for the η field (the analog of Eq.(3.13)) and the internal-spacial components of the gauge potential $A_i, \forall i \in \{3,4,5\}$ (the analog of Eq.(3.12)) are automatically fulfilled. But the equation of motion for the time-component of the gauge potential A_t demands an additional condition to hold, which turns out to be the celebrated Born-Infeld equation on the electric field strength:

$$\nabla \cdot \left(\frac{\vec{E}}{\sqrt{1-|\vec{E}|^2}} \right) = 0. \tag{3.16}$$

Therefore, the solution can be reformulated as the problem of finding the Born-Infeld electrostatic solutions.

The on-shell Lagrangian density, the sum of Eq.(3.14) and Eq.(3.8), can be further simplified using the relation Eq.(3.15):

$$\mathcal{L}^{OnShell} = \sqrt{1-|E|^2}. \tag{3.17}$$

Notice that the on-shell Lagrangian density only depends on the electric field strength $\vec{E}$, but not on the boundary embedding function ϕ. The simplest analytic solution to this equation of motion is that of a single point charge located at the origin,

$$\vec{E} = \frac{Q}{\sqrt{{r_3}^4 + Q^4}}\hat{r}_3, \tag{3.18}$$

with an electric field decaying with the usual $1/r$ at large distances but reaching a finite value at small r. For the special case that no magnetic fields (and hence no ϕ field) are turned on, this finite-density solution matches the analytic solution previously studied e.g.

in [62, 63]. Supersymmetry is explicitly broken in these solutions. On the field theory side, this is due to the presence of a finite chemical potential. The free energy is negative. What our solution shows is that even in the presence of this finite density, we still have the full moduli space of half-D3 branes ending at arbitrary positions r_i we found in the zero density supersymmetric vacuum. A typical configuration of this type is displayed in panel (b) of figure 3.1. Irrespective of the position of the D3-brane spikes, the free energy of the system is always given by the expressions found in [62], as long as the electric field is given by the simple BIon like solution Eq.(3.18).

Note that, as in the last subsection, further progress can be made in the spherically symmetric case, that is when ϕ and $\vec{B}$ are due to a single source at the origin. In this case the magnetic field once more is simply given by a constant flux through the internal S^2. One obtains coupled ordinary differential equations for $A_t(r)$ and $\phi(r)$ which can be integrated as both fields only appear derivatively in the action. One can easily reproduce the interesting feature that the free energy, at zero temperature, is complete independent of the magnetic flux through the sphere and only depends on the baryon number chemical potential, that is the electric flux. In this special case one can also find the finite-temperature embeddings [1].

This intriguing presence of supersymmetric-broken moduli space demands further investigation. What is perhaps even more interesting is to study other solutions of the Born-Infeld equations corresponding to multiple separated electric charges. These multiple-BIon solutions and their implication for stability will be the main topic for the next section.

3.4 DBI Solutions Revisited and the Stringy Interpretations

The ansatz we constructed in the last section reduces the full set of nonlinear coupled equations of motion into the single Born-Infeld equation, Eq.(3.16), allowing us to explore the dynamics of the probe brane world volume gauge field. It is well known that no non-trivial global regular solutions of Eq.(3.16) do exist, see e.g. [64]. To show this, one first observes that solutions of Born-Infeld electrostatic can be shown, by the level curve technique, to be the same as maximal hypersurfaces in Minkowski spacetime. For latter a theorem exist (the

[1] These solutions have been worked out in collaboration with Andy O'Bannon and will potentially appear elsewhere.

Minkowski version of the original Bernstein theorem) saying that the regular solutions can only be trivial. Therefore, to introduce the non-trivial electric field strength, we will need to modify the right hand side of the Eq.(3.16) by explicitly including source terms. We have not introduced any charged fields in the bulk theory. So all such sources have to either sit behind the horizon or at spatial infinity, that is at infinite x_3 in the AdS spacetime.

The simplest non-trivial solution is given by a single BIon, Eq.(3.18). We needed to introduce a single point charge Q in order to support this solution. This charge is located at $r = 0$, which corresponds to the horizon in the AdS geometry. As in most holographic finite-density studies, the electric field of the single-BIon is sourced by a charged horizon. Standard lore has it that this corresponds to charges carried by fractionalized charge carriers in the field theory [65]. The corresponding gauge potential A_t approaches an asymptotic constant at the boundary, dual to the chemical density of the associated vacuum state in the dual gauge theory description of AdS/CFT dictionary.

Multiple-BIon solutions exist due to general existence theorem as well, even though the explicit solutions have not been analytically proposed yet [64]. Such multiple-BIon solutions must be supported by electric point charges located at some locations r_a, where a runs over the point charges in the multiple-BIon solution. Naively this requires us to introduce point sources inside AdS space. Note however that as long as we chose all the r_a to coincide with some of the D3-brane spikes, that is with some of the r_i introduced above, we effectively pushed these charges off to infinite x_3. Schematically such a solution is depicted in panel (c) of figure 3.1. Note that the magnetic charge q_i of the spikes is completely unrelated to the electric charge Q_a. Former measures how many D3 branes end on the D5 brane, latter measures how many F1s are dissolved in it. In the field theory side, these configurations correspond to finite baryon number on the defect sourcing a free $U(1)$ factor associated with the half-D3 brane. So such multiple-BIon solutions can easily be realized in our setup.

Furthermore, in [64], Gibbons argued that the single BIon, with macroscopic charge, is actually unstable against fission, based on a scaling relation between the energy and charges of the BIons. This fission of the macroscopic BIon may signal an instability of the finite-density brane system with all charges behind the horizon. Combining our result that the on-shell action of the brane system reduces to the BI action with the scaling arguments

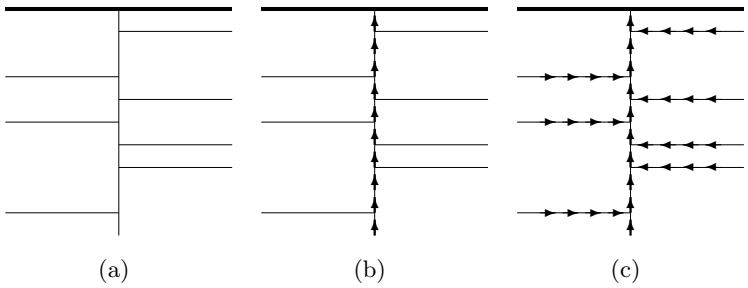

Figure 3.1: Three Different scenarios: (a) Pure Magnetic Flux; (b) A Single BIon; (c) Multiple BIons

of [64] demonstrates that the free energy of a system of fixed baryon number Q_{tot} is lower if the charge is not carried by the horizon but instead is supported by D3 brane spikes. The configuration can clearly lower its free energy by disintegrating the central stack of D3 branes and letting the probe branes carry the finite density. That is, the system has lower free energy on its Higgs branch. It is not clear to us whether this necessarily needs to be interpreted as an instability. In the process of pulling a single probe D3 brane out of the horizon and letting it support part (or all) of the electric flux of the horizon we change the boundary conditions on the Maxwell $U(1)$ electric field at spatial infinity. It would be very interesting to do a linearized analysis of fluctuations along the lines of [59] for the finite-density D3/D5 system to see if this instability towards disintegration of the central D3 brane stack is visible at the perturbative level.

3.5 Conclusion

In this chapter, we present an ansatz for the D3/D5 probe brane system with non-trivial magnetic D5 worldvolume gauge field strength. The ansatz turns out to satisfy a no-force condition, signaling preserved supersymmetry. These brane configurations reproduce the full Higgs branch moduli space of the holographically dual supersymmetric defect conformal field theory. Within this sector, we find that probe brane system dual to the finite-density vacuum, based on the scaling argument from in [64], can lower its free energy by fissioning.

This potentially signals an instability whose precise nature will be left to future research.

Chapter 4

ENTANGLEMENT ENTROPY FOR PROBE BRANES

In this chapter, we recollect our previously published work, in collaboration with Prof. Andreas Karch, "Entanglement Entropy for Probe Branes" on Journal of High Energy Physics, vol.1401, p.180, 2014 [3], in which we give a prescription for calculating the entanglement entropy in holographic probe brane systems by systematically taking the leading order backreaction of the probe brane into account. We find a simple compact double integral formula, which is insensitive to many details of the backreaction, most notably the internal space or the non-metric fields sourced by the probe. We validate our method by comparing to exact results in solvable toy models. We also determine the entanglement entropies for a sphere and a strip in the top-down D3/D7 and D3/D5 system. For the sphere the entanglement entropy has also been obtained by other methods and we find perfect agreement.

The organization of the chapter is as follows: In Sectin 4.1, we recapitulate the relevant background for the program of holographical calculations for quantum entanglement entropy; In Section 4.2, we review the basic definition of a probe brane system and derive our basic formula; In Section 4.3, we introduce two simple solvable toy models in which the backreaction can easily be taken into account, which we use later to validate our results. In Section 4.4, we show that, due to the special properties of the entangling surface, in many cases the deformation of the internal space due to the backreaction can be neglected. This allows us to map several top-down probe brane systems, with known field theory dual, to the results obtained in the two solvable toy models; In Section 4.5, we apply our formalism to the toy models of Section 3 and hence, by the results of Section 4.4, also to two well-studied top-down models. We find perfect agreements with the fully backreacted answer for the toy models; In Section 4.6, we demonstrate the perfect agreement with results obtained by Jensen and O'Bannon [66] using an alternative method based on the Casini-Huerta-Myers "trick" [66, 67].

4.1 Introduction

Entanglement entropy (EE) has emerged as a very powerful theoretical tool in the studies of topological phases of matter, strongly correlated systems in general and even the quantum nature of gravity. A large class of strongly coupled field theories in which EE can be calculated reliably is provided by holography [21, 20, 22]. Ryu and Takayanagi (RT) introduced in [68] a very simple prescription for how to calculate the EE in field theories with a holographic dual. To specify the EE in a field theory with $d-1$ spatial dimensions, one needs to pick a $d-2$ dimensional entangling surface, Σ, separating (at a given time t) the degrees of freedom of the field theory into two subsystems A and B. By tracing over the degrees of freedom in B, one obtains a reduced density matrix for the degrees of freedom in A and vice versa. Even when describing a pure state, the reduced density matrices are mixed due to the loss of information inherent in tracing over a subspace. The standard von Neumann entropy associated with the reduced density matrix is the entanglement entropy. For a zero temperature state, the entanglement entropies associated with subsystems A and B respectively are identical. This entanglement entropy provides a measure of the entanglement present in the original state of the full system. The RT proposal asserts that, in the holographic dual description, the EE is given by

$$S_A = \underset{\{\gamma_A|_{\partial\gamma_A=\Sigma}\}}{\text{Min}} \frac{\text{Area}(\gamma_A)}{4G_N}, \tag{4.1}$$

where G_N is Newton's constant and the γ_A, whose area determines the EE, is a minimal area surface in the holographic bulk, terminating on the prescribed entangling surface Σ on the boundary. In the field theory, one important contribution to the EE is the short range entanglement of the degrees of freedom in the vicinity of the entangling surface. This contribution is sensitive to the details of the short distance physics and is proportional to the area of the entangling surface. In addition to this UV divergent area term, there are several subleading terms, some of which carry universal information about the long range entanglement in the state. Especially in the case of conformal theories, the structure of these terms has been clarified by the holographic calculations. For a recent review on these developments see [69].

In this work we give a derivation of the holographic EE for a large class of holographic theories for which so far application of the RT formula has been mostly unsuccessful: probe brane systems [35, 36]. Probe brane setups describe strongly coupled field theories with special properties. Not only does one need to take a "large N" limit which guarantees a classical dual, one also needs two sectors which scale as different positive powers of N. One common class of examples are large N gauge theories with order N^2 gluon degrees of freedom coupled to fundamental representation quarks with order N degrees of freedom. In this case, the quarks are still classical, but they act as probes of the glue background: their dynamics adjusts itself to the strongly interacting background provided by the glue, but does not backreact on it.

Probe brane systems have been studied in many different contexts. In applications of holography to nuclear physics, the most successful holographic cousin of QCD, the Sakai-Sugimoto model [48], is based on a probe brane system. For applications to condensed matter physics, probe brane setups can realize a variety of interesting situations. The glue degrees of freedom can act as a heat-bath for the quarks, giving the simplest realization of a model which allows for dissipation and hence a finite DC conductivity [70]; the properties of such a system can be engineered to be in qualitative agreement with that of high-T_c superconductors in the strange metal phase [43]. Probe branes give straight forward realizations of holographic lattices [71], including holographic realizations of a Kondo-lattice, giving a controlled field theory example of a non-Fermi liquid [72]. Non-Landau phase transitions with an exponential scaling of the order parameter close to the critical point are also easy to realize via probes [73]. Probe brane systems also can realize novel phases of compressible matter with peculiar properties: they can display a zero sound pole characteristic of Fermi liquids despite an unusual temperature dependence of the heat capacity [63, 74, 75]; they can display the appearance of a moduli space despite the absence of any supersymmetry [2, 76]; maybe most interestingly in the current context, they can realize non-relativistic critical points with hyperscaling violating exponent $\theta = d - 2$ [77]. This particular value has been argued in [78, 79] to be associated with a logarithmic enhancement of the area law for the EE. It would be extremely interesting to see if the well-understood field theory provided by the probe brane system of [77] bears out this expectation. Last but not

least, probe brane systems have been instrumental in giving a holographic realization of many non-trivial topological phases, such as the quantum Hall effect [80] and fractional topological insulators [81]. Non-trivial entanglement is a hallmark of topological states, so calculating the EE in these systems should be a worthwhile exercise.

In principle the RT formula can immediately be applied to probe branes. Even though to leading order in a large N expansion the effect of the stress-energy carried by the probe can be completely neglected, one can systematically incorporate the backreaction of the probe brane on the background geometry by solving Einstein's equation in a $1/N$ expansion with the probe-source included. To get the contribution of the probe degrees of freedom to the EE, one simply needs to re-solve the minimal area problem in this fully backreacted metric and then directly apply the RT prescription eq.(4.1). For simple toy models [82] and highly supersymmetric cases with "fat branes" realized as a scalar lump [83], this procedure has been carried out explicitly for the fully backreacted metric. In this work, we are going to derive a simple compact formula for the leading order contribution of the probe to the EE following this general strategy. Note that our formula therefore directly follows from the RT prescription and is not a separate conjecture. We write our final answer for the EE as a double integral involving a gravitational Green's function, eq.(4.11). This is the main result of this work. We validate our integral expression by comparing to two solvable toy models. In the process we have to understand the UV divergences in our integral and describe their physical origin and meaning. We can also immediately deduce from our integral expression that the expressions for the EE in our two bottom-up toy models in fact also applies to two of the most studied probe brane systems in type IIB supergravity despite the complications associated with the internal space.

4.2 The Entanglement Entropy of probe branes

4.2.1 General Probe Brane Systems

The generic probe brane setup has a bulk action which includes a Einstein-Hilbert term coupled to a matter Lagrangian[1],

[1]In here and in the following we denote the dimension of the bulk spacetime as $d+1$. The dual field theory has d spacetime dimensions. If the bulk gravity solution also has an internal factor we refer to

$$S_{bulk} = \frac{1}{16\pi G_N} \int d^{d+1}x\sqrt{-g}\,\left(R + \mathcal{L}_{bulk}\right), \tag{4.2}$$

and a probe brane action, which typically starts with a tension term, that is a uniform energy per unit volume

$$S_{probe} = T_0 \int d^{n+1}z\,\sqrt{-g_I}\mathcal{L}_{probe} = T_0 \int d^{n+1}z\,\sqrt{-g_I}\,(1 + \ldots)\,. \tag{4.3}$$

Here $\sqrt{g_I}$ denotes is the induced metric on the $n+1$ dimensional worldvolume. The matter in the bulk action should allow for a spacetime with a holographic interpretation characterized by a curvature radius L. The simplest example is a pure negative cosmological constant giving rise to an AdS_{d+1} vacuum solution. In this case the dual conformal field theory (CFT) however is not known explicitly. For examples, where the dual field theory is known from the embedding of the duality in string theory, the bulk matter sector is typically more complicated: the gravitational $\mathrm{AdS}_5 \times S^5$ background dual to $\mathcal{N} = 4$ SYM is accompanied by a constant 5-form flux field strength. The brane action can be almost arbitrary. For D-brane probes one typically has, in addition to the tension term, a Maxwell term for a worldvolume gauge field dual to the conserved particle number on the field theory side. The action in this case contains higher powers of the field strength as well, which are known to sum up into the form of Dirac-Born-Infeld (DBI) action. The important property of a probe brane setup is the following hierarchy of scales:

$$\frac{L^{d-1}}{G_N} \gg T_0 L^{n+1} \gg 1 \tag{4.4}$$

$L/G_N^{1/(d-1)}$ is the curvature radius in Planck units. This quantity appears as an overall prefactor of the bulk action. It being large allows us to approximate quantum gravity in

---

spacetime as the lower dimensional space one obtains after compactification. The worldvolume of the probe brane has $n+1$ spacetime dimensions, where clearly $n \leq d$. For the bulk we use coordinates x^μ with $\mu = 0, \ldots, d$, and for the worldvolume of the probe brane z^i with $i = 0, \ldots, n$. Last but not least, the entangling surface in the field theory has $d-2$ spatial dimensions and is completely localized in time. In the holographic dual the EE associated with this entangling surface is dual to a $d-1$ dimensional extremal area for which we use coordinates w^a with $a = 0, \ldots, d-2$. As we will be mostly interested in static geometries we reserve the superscript ^{0} for the radial coordinate, not time, as is common in the literature on gravitational propagators on Anti de-Sitter (AdS). Time is the coordinate with the largest label (x^d and z^n; w only runs over spatial coordinates). We'll denote by $\vec{x}^2$, $\vec{w}^2$ and $\vec{z}^2$ the contractions of the non-zero indices with a Kronecker delta (when working in Euclidean signature) or an η tensor (when working in Lorentzian signature).

the bulk by the semi-classical saddle point, that is by the solution to the classical equations of motion. Similarly $T_0 L^{n+1}$ appears as the overall prefactor of the probe brane action. It being large ensures that the probe brane action can be treated classically as well. Last but not least, the combination $G_N T_0 L^{n-d+2}$ controls the strength with which the brane stress tensor appears as a source on the right hand side of Einstein's equations (and similarly it controls how much other bulk fields are sourced by the brane). It therefore sets the size of the backreaction of the brane on the background geometry. To leading order, the brane simply is a probe that minimizes its own worldvolume action in a fixed background geometry. The backreaction can systematically be calculated in an expansion in the small dimensionless parameter

$$t_0 \equiv 16\pi G_N T_0 L^{n-d+2}. \tag{4.5}$$

In the field theory, probe brane systems describe setups where we have two different classical sectors (that is sectors which a large number of degrees of freedom) with a hierarchy between them. One large class of examples including [36, 35, 48] coupling fundamental matter to a large N gauge theory. In this case typically $L^{d-1} G_N \sim N^2$, as there are order N^2 glue degrees of freedom, and $T_0 L^{n+1} \sim N$, as there are of order N degrees of freedom in the fundamental matter. The order N^2 and N pieces in physical quantities like the free energy or, of interest here, the EE are determined by classical physics. These "flavor" probe branes are not the only examples that display such a hierarchy of scales. Another important example is the fundamental F1 string: here $n = 1$ and $T_0 L^2 \sim \sqrt{\lambda}$ where λ is the 't Hooft coupling of the dual gauge theory, which also needs to be taken large in the large N limit for a good supergravity description to exist in that case.

4.2.2 Calculating the EE for probe branes

In principle, the EE for Einstein gravity coupled to brane sources directly follows from the RT formula. One needs to calculate the full backreaction of the probe brane, and then re-solve the minimal area problem for the EE in the fully backreacted geometry. In the probe limit this calculation should however simplify dramatically. We only need the leading order backreaction of the brane on the background geometry, and then calculate the change

in area of the minimal area defining the EE in the original background due to this small change in the background metric.

In terms of the probe-brane stress tensor

$$T^{\mu\nu}_{probe} = \frac{2}{\sqrt{-g_I}} \frac{\delta\left(\sqrt{-g_I}\mathcal{L}_{min}\right)}{\delta g_{\mu\nu}}\bigg|_{x^\mu \to x^\mu_P(z^i)}, \tag{4.6}$$

where $x^\mu_P(z^i)$ describes the embedding of the probe, the backreacted metric to leading order in the backreaction can be written as

$$(\delta g)_{\mu\nu} = (8\pi G_N T_0) \int d^{n+1}z \, \sqrt{g_I}\, G_{\mu\nu\rho\sigma} T^{\rho\sigma}_{probe}, \tag{4.7}$$

where $G_{\mu\nu\rho\sigma}$ is the appropriate Green's function of linearized Einstein gravity. For static backgrounds, which we will be mostly concerned with, one can use the Euclidean signature geometry and use the unique Green's function that is regular inside the holographic space-time and obeys Dirichlet boundary condition at the boundary. For pure AdS, this Green's function has been determined in a very convenient form in [84]; we'll review the construction in detail when discussing specific examples in the following sections. For time-dependent backgrounds we should use the retarded Green's function.

The minimal area is described by an embedding $x^\mu_M(w^a)$ which can be derived from an "action"

$$S_{min} = \frac{1}{4G_N} \int d^{d-1}w \, \sqrt{\gamma} \equiv \frac{1}{4G_N} \int d^{d-1}w \, \mathcal{L}_{min}, \tag{4.8}$$

where γ is the determinant of the induced metric. The EE according to the RT formula is now simply the on-shell value of this action. Note that while RT was originally derived for static backgrounds, it has been argued in [85] that in the time-dependent case the EE is still given by an extremal surface and so the action eq.(4.8) still applies in this case. The on-shell Lagrangian for the minimal surface depends both on the embedding function $x^\mu_M(w^a)$ and the background metric. To calculate the change in the EE due to the backreaction of the brane we can hence write

$$\delta S_{min} = \frac{1}{4G_N} \int d^{d-1}w \, \sqrt{\gamma} \left(\frac{T^{\mu\nu}_{min}}{2} (\delta g)_{\mu\nu} + \frac{\delta \mathcal{L}_{min}}{\delta x^\mu_M} \delta x^\mu_M \right). \tag{4.9}$$

Similar to the probe brane we have defined the "stress tensor"

$$T^{\mu\nu}_{min} = \frac{2}{\sqrt{-\gamma}} \frac{\delta\left(\sqrt{-\gamma}\mathcal{L}_{min}\right)}{\delta g_{\mu\nu}}\bigg|_{x^\mu \to x^\mu_M(w^a)}. \tag{4.10}$$

For the minimal area surface, the stress tensor is proportional to the variation of the determinant of the induced metric. For the probe brane we expect such a term to be present as well due to the standard tension term, but extra contributions, e.g. due to the worldvolume gauge fields, are also allowed.

δS_{min} can be simplified dramatically by noting that $\frac{\delta \mathcal{L}_{min}}{\delta x^{\mu}_{M}}$ vanishes when evaluated on the unperturbed minimal area due to the equations of motion[2]. Plugging in our expression eq.(4.7) for the perturbed metric we arrive at the following compact expression of the entanglement entropy

$$S_A = (\pi T_0) \int (d^{d-1}w\sqrt{\gamma})\,(d^{n+1}z\sqrt{g_I})\left(T^{\mu\nu}_{min} G_{\mu\nu\rho\sigma} T^{\rho\sigma}_{probe}\right). \tag{4.11}$$

This simple double integral gives the EE for a generic probe brane system. It can be thought of as the gravitational potential energy between the probe brane and the "energy density" of the minimal area surface. The formula is valid as long as the only source of δg, to leading order in t_0, comes from the stress tensor on the probe brane. If the probe brane sources bulk fields other than the metric, there are additional contributions one needs to worry about. If we denote bulk fields other than the metric (e.g. the p form potentials of type IIB supergravity) collectively by Φ_{bulk}, the backreaction of the flavors will induce $\Phi_{bulk} \sim t_0$ together with $\delta g \sim t_0$ for all the Φ_{bulk} that are sourced by the brane. For example, a Dp brane in IIB supergravity will source the dilaton and the $p+1$ form Ramond-Ramond gauge field it is charged under. If the bulk stress-energy tensor has a term linear in Φ_{bulk}, this order t_0 change in Φ_{bulk} drives a change in the metric that is also of order t_0 and would have to be included. Fortunately, the Einstein-frame stress tensor for, say, type IIB supergravity is quadratic and higher order in fields, so the stress tensor is at least quadratic in Φ_{bulk} and so this "secondary" effect on the metric due to the other brane sources is negligible. The only exception to this statement arises if we are studying a background in which Φ_{bulk} is turned on before we add the probe brane. In this case, even though the stress tensor is quadratic in the full Φ_{bulk}, there is a term linear in the probe-sourced $\delta\Phi_{bulk}$ when combined with a background Φ_{bulk}. As an example, in the $AdS_5 \times S^5$ solution dual to $\mathcal{N} = 4$ supergravity,

[2]This fact has also recently been observed in [86, 87] who also studied the response of the EE to small metric perturbations.

the background has a non-trivial 4-form gauge field C_4 turned on. Correspondingly, our formula does not apply to branes that source C_4. For D7 branes and D5 branes without worldvolume gauge fields our formula is applicable; however, for D3 branes, D5 brane with non-vanishing F and D7 branes with non-vanishing $F \wedge F$, potentially it is not[3]. Another case in which our analysis does not apply due to secondary backreaction is a D6 brane probe [88, 89, 90, 91, 92] in ABJM [93] (the D6 sources the 2-form RR field strength, which in ABJM has a non-trivial background).

The Green's function in the expression above falls off sufficiently fast near the boundary to ensure that the above integral is finite for sources that do not extend out to the boundary. However, most examples of probe branes of interest *do* involve probe branes extending all the way to the boundary. This is the case whenever the probe brane describes the addition of matter to the boundary field theory, such as in the D3/D5 system [36], the D3/D7 system [35] or the Sakai-Sugimoto model [48]. Probe branes completely localized in the bulk of the holographic spacetime, such as e.g. a single D3 brane probe[4] at a fixed radial position in $AdS_5 \times S^5$ or the D7 brane dual to the quantum Hall effect of [80], correspond to states of the dual field theory. While in the latter case of a radially localized probe the z integral is UV finite, the more interesting case of a probe extending to the boundary has a divergence in the z integral that needs to be tamed. In addition, the minimal area defining the EE always extends all the way to the boundary. Correspondingly its "stress tensor" doesn't fall off near the boundary and so the w integral is always UV divergent and needs to be regulated. This UV divergence is physical, capturing the underlying structure of the entanglement. Like the leading divergence of EE itself, the correction to the EE due to the probe brane is sensitive to short distance physics as it is dominated by the short range entanglement of

[3]The stress tensor associated with C_4, written in terms of $H_5 = dC_4$, has terms of the structure $H_{\mu\cdots}H^{\cdots}_{\nu}$ and of the structure $g_{\mu\nu}H^2$. Since the background metric is diagonal, the C_4 sourced by the brane needs to share at least 3 indices with the background C_4 to have a chance to contribute a non-trivial term to the stress tensor at order t_0. For example, the interesting case of a D5 with a field strength $F \propto dr \wedge dt$ turned on along the worldvolume (corresponding to the finite density holographic quantum liquid of [63]) sources C_4 with two legs along the AdS direction and two legs in the internal space. Since the background C_4 only has components either entirely in the internal space or entirely in AdS, this particular worldvolume field strength does not give an order t_0 term in the stress tensor and so is compatible with our formula even though C_4 is sourced.

[4]As a D3 brane probe sources C_4 in this particular instance our formula wouldn't apply to begin with. See the discussion in the preceding paragraph.

nearby probe degrees of freedom. We'll discuss both these UV sensitivities in more detail below when we look at explicit examples.

4.3 Two simple solvable examples

There are two simple examples documented in the literature where the full backreaction of a toy model of probe brane can be given in a simple closed-form expression and hence one can easily calculate the full entanglement entropy, not just in the probe limit. We will use the exact answers in these two examples to validate our method. Both are based on the simplest holographic bottom-up action which is not directly obtained from string theory and correspondingly the dual field theory is not explicitly known. The gravitational action in both cases is simply Einstein gravity with a negative cosmological constant in $d+1$ dimensions:

$$S = \frac{1}{16\pi G_N}\int d^{d+1}x\sqrt{g}\left(R + \frac{d(d-1)}{L^2}\right). \tag{4.12}$$

The vacuum solution for this action is AdS_{d+1} with curvature radius L. We write the metric on AdS_{d+1} as

$$ds^2 = \frac{L^2}{(x^0)^2}\delta_{\mu\nu}dx^\mu dx^\nu, \tag{4.13}$$

where the reader should keep in mind that x^0 is the (spatial) radial coordinate. $\eta_{\mu\nu}$ is mostly plus and has -1 as its last diagonal entry. For static configuration we will often be interested in Euclidean AdS in which case $\eta_{\mu\nu}$ is replaced with $\delta_{\mu\nu}$. The probe brane action only has the standard tension term

$$S_{probe} = -T_0\int d^{n+1}z\,\sqrt{g_I}, \tag{4.14}$$

where $\sqrt{g_I}$, as before, is the induced metric on the $n+1$ dimensional worldvolume. The two special cases we will be considering are $n = d$ (a spacetime filling probe brane) and $n = d-1$ (a codimension-1 probe brane).

4.3.1 Spacetime filling probe branes

The case of a spacetime filling probe ($n = d$) has been studied in detail in [53] as an exactly solvable model for probe branes. The important point here is that a spacetime filling brane

of this type simply corresponds to a shift in the cosmological constant and hence the exact solution is again AdS_{d+1} with a shifted curvature radius l given by [53]

$$l = L\left(1 + \frac{t_0}{2d(d-1)}\right). \tag{4.15}$$

This can be rewritten as a first-order shift in the metric

$$(\delta g)_{\mu\nu} = \frac{t_0 L^2}{d(d-1)} \frac{\delta_{\mu\nu}}{(x^0)^2}. \tag{4.16}$$

For any entangling surface the EE in the full spacetime geometry can be obtained from the one in the original AdS by implementing the simple change eq.(4.15).

4.3.2 Codimension-1 "RS" type probe branes

For $n = d - 1$ the simple bottom-up model reduces to the famous Randall-Sundrum setup [94, 95]. Depending on the tension, the defect worldvolume can be AdS, dS or Minkowski space. In the probe limit we are always automatically in the limit of an "undercritical" tension, where the small tension of the brane gives a negligible contribution to the induced cosmological constant on the brane and so the worldvolume is AdS. This scenario has been shown to be dual to a conformal field theory with defect or boundary in [36]. The EE for this model in $d = 2$ has been calculated in [82]. For all RS (that is codimension-1) setups the fully backreacted spacetime metric can be easily found using the Israel junction equations [96]. As the sources are delta-function localized, the spacetime can be taken to be a slice of AdS on both sides of the defect. These two spaces will be glued together across the location of the brane. Of course the metric should be continuous across the interface, but it's first derivative however will not be, due to the delta function source. Integrating Einstein equations across the defect, one finds that the jump in the extrinsic curvature is given by the brane stress tensor,

$$(K_{ij} - g_{ij}K)|_{r-\epsilon}^{r+\epsilon} = 8\pi G_N T_{ij}, \tag{4.17}$$

where r is the coordinate normal to the hypersurface of the brane and ϵ, as usual, is an infinitesimally small positive number. To find a solution to the Israel jump equation it is

easiest to write AdS_{d+1} in AdS_d slicing:

$$ds^2 = dr^2 + \cosh^2\left(\frac{r-c}{L}\right) ds^2_{AdS_d}. \tag{4.18}$$

Here $ds^2_{AdS_d}$ denotes the metric on an AdS_d with curvature radius L. For a globally AdS_{d+1} spacetime the constant c can be absorbed by shifting the r coordinate. For the RS setup it is however convenient to use c to locate the brane hypersurface at $r = 0$. The piecewise AdS geometry, that is the fully backreacted solution in response to the brane source, can now be written as

$$ds^2 = dr^2 + \cosh^2\left(\frac{|r|-c}{L}\right) ds^2_{AdS_d}. \tag{4.19}$$

Clearly this is locally AdS_{d+1} away from $r = 0$. At $r = 0$ the jump equation reads

$$\frac{2(d-1)}{L}\sinh\left(\frac{c}{L}\right) g_{ij}^{AdS_d} = 8\pi G_N T_{ij} = 8\pi G_N T_0 \cosh\left(\frac{c}{L}\right) g_{ij}^{AdS_d}, \tag{4.20}$$

where in the last step we used that the matter action is given by eq.(4.14). The Israel jump condition hence gives us c in terms of the tension as

$$t_0 = 4(d-1)\tanh\left(\frac{c}{L}\right) \approx \frac{4(d-1)c}{L}. \tag{4.21}$$

In the last step we used that in the probe limit t_0 and hence c are small, so the hyperbolic tangent function can be approximated by its argument. The first equality in eq.(4.21) however is exact even away from the probe limit. In the probe limit we can write the change in the metric as

$$\delta g = -\frac{c}{L}\sinh\left(2\frac{|r|}{L}\right) ds^2_{AdS_d} = -\frac{t_0}{4(d-1)}\sinh\left(2\frac{|r|}{L}\right) ds^2_{AdS_d}. \tag{4.22}$$

To perform calculations in the AdS_{d+1} background in the standard coordinate system used in eq.(4.13), one can transform δg into the x^μ coordinates of eq.(4.13). Parametrizing the AdS_d metric as

$$ds^2_{AdS_d} = L^2\left(\frac{dy^2 + d\vec{x}^2}{y^2}\right), \tag{4.23}$$

where $\vec{x}$ stands for $x^2, \ldots, x^d$, we see that the two coordinate systems given in eq.(4.13) and eq.(4.18) (for $c = 0$) are related to each other by the following change of coordinates:

$$x^0 = \frac{y}{\cosh(r/L)}, \qquad x^1 = y\tanh(r/L). \tag{4.24}$$

Applying the same change of coordinates to δg allows us to write its components in the x^μ coordinate system as

$$(\delta g) = -\frac{L^2 t_0}{2(d-1)(x^0)^2} \frac{|x_1|}{\sqrt{(x^0)^2+(x^1)^2}} \left(d\vec{x}^2 + \frac{(x^1 dx^1 + x^0 dx^0)^2}{(x^0)^2+(x^1)^2} \right). \tag{4.25}$$

4.4 Internal space

In the last section we introduced two toy models with the motivation of providing gravity-plus-probe systems allowing exact determination of the EE to all orders in the backreaction. We need these examples in order to validate our method. Probes with a known string embedding are typically much more complicated. For example, the well-studied D3/D7 [35] and D3/D5 [36, 37] systems correspond to codimension-2 and codimension-4 branes respectively wrapping an $\mathrm{AdS}_5 \times S^3$ or $\mathrm{AdS}_4 \times S^2$ submanifold in an $\mathrm{AdS}_5 \times S^5$ background geometry. Their backreaction will induce a change in the full 10 dimensional geometry with non-trivial dependence on the internal S^5 coordinates. The fully backreacted solutions have been worked out for the D3/D7 system in [97] and for the D3/D5 system in [98, 99, 100]. While available, these fully backreacted solutions are rather complicated and working out solutions to the minimal area problem relevant for the EE in these backgrounds is cumbersome.

As we will explain in more detail here, our general result eq.(4.11), for the leading order correction to the EE in the probe expansion, allows us to demonstrate that the answers we obtain in the toy models are, in fact, valid for a large class of branes which are non-trivially embedded into the full 10 (or higher) dimensional space-time. In particular, the EE calculation for the D3/D7 system (to leading order in t_0) can be mapped exactly to our codimension-0 toy model, whereas the EE for the D3/D5 system (again to leading order in t_0) can be mapped to the codimension-1 toy model. To this order, the fully backreacted solutions of [97, 98, 99, 100] are not needed.

To prove this assertion, we need to use the representation of a Green's function as a sum over eigenfunctions. The Green's function $G_{\mu\nu\mu'\nu'}$ of (trace reversed) linearized Einstein

gravity obeys a differential equation,

$$\mathcal{W}_{\mu\nu}{}^{\lambda\rho}G_{\lambda\rho\mu'\nu'} = \left(g_{\mu\mu'}g_{\nu\nu'} + g_{\mu\nu'}g_{\nu\mu'} - \frac{2}{d-1}g_{\mu\nu}g_{\mu'\nu'}\right)\delta(x,x') + D_{\mu'}\Lambda_{\mu\nu\nu'} + D_{\nu'}\Lambda_{\mu\nu\mu'}, \tag{4.26}$$

where $\delta(x,x')$ is the appropriate curved space Dirac delta function. Here $\mathcal{W}_{\mu\nu}{}^{\lambda\rho}$ is a linear second order differential operator acting on rank-2 tensors $h_{\mu\nu}$. Its detailed form can be found in any standard textbook and will not be important for our argument. In the example of AdS_{d+1} that will be of most interest to us below, we have [84]

$$\mathcal{W}_{\mu\nu}{}^{\lambda\rho}h_{\lambda\rho} = -D^\sigma D_\sigma h_{\mu\nu} - D_\mu D_\nu h^\sigma_\sigma + D_\mu D^\sigma h_{\sigma\nu} + D_\nu D^\sigma h_{\mu\sigma} - 2(h_{\mu\nu} - g_{\mu\nu}h^\sigma_\sigma). \tag{4.27}$$

The pure diffeomorphism terms on the right hand side of eq.(4.26), represented by $\Lambda_{\mu\nu\mu'}$, can be eliminated by a coordinate transformation on the primed coordinates. With appropriate boundary conditions $\mathcal{W}_{\mu\nu}{}^{\lambda\rho}$ is a hermitian operator and so its eigenfunctions form a complete orthonormal basis[5].

For product manifolds these eigenfunctions factorize mode by mode. Let us first exhibit the consequences of this factorization for the simpler example of a scalar field. In that case the analog of eq.(4.26) reads

$$WG(x,x') = \delta(x,x'), \tag{4.28}$$

where W this time is simply the (curved space) Laplacian. For the product manifold we can write

$$W = W^S + W^I, \tag{4.29}$$

where $W^{S/I}$ only acts on the spacetime/internal part. One can obtain a representation of G by first solving the eigenvalue problem for W:

$$W\psi^S_m(x_S)\psi^I_n(x_I) = (E_m + E_n)\psi^S_m(x_S)\psi^I_n(x_I). \tag{4.30}$$

Here $x_{S/I}$ collectively stand for all the coordinates in the spacetime/internal factor of the product manifold, and we already employed a separation of variables ansatz for the eigen-

[5]This is certainly true for the Euclidean operator, which is appropriate for static calculations as we perform here. For time-dependent backgrounds one typically imposes purely in-falling boundary conditions [101] at the horizon ruining the Hermiticity of $\mathcal{W}_{\mu\nu}{}^{\lambda\rho}$. Correspondingly, our arguments here may not be applicable to the retarded Green's function in that case.

functions:

$$W^S\psi^S_m(x_S) = E_m\psi^S_m(x_S), \qquad W^I\psi^I_n(x_I) = E_n\psi^I_n(x_I), \tag{4.31}$$

where n and m are labeling the eigenmodes. One particular mode that will play an important role in what follows is the zero mode of the internal space. The constant function $\psi^I_0 = V_I^{-1/2}$, where V_I denotes the volume of the internal manifold, is clearly annihilated by the Laplacian and so is an eigenfunction with eigenvalue $E_0 = 0$.

Since the eigenfunctions of the hermitian operator W form a complete orthonormal basis, we can immediately write

$$G(x_S, x_I, x'_S, x'_I) = \sum_{n,m} \frac{\psi^S_m(x_S)\psi^S_m(x'_S)\psi^I_n(x_I)\psi^I_n(x'_I)}{E_n + E_m}. \tag{4.32}$$

This representation of G is of huge help when integrating against sources which themselves factorize. In particular, if the source $T(x_S, x_I)$ is constant as a function of the internal directions, we can write $T(x_S) = V_I^{1/2}\psi^I_0(x_I)T(x_S)$. When integrating T against G, orthonormality of the modes now picks out the corresponding zero mode from the Green's function:

$$\int_{x_S,x_I} \sqrt{g}\, G(x_S, x_I, x'_S, x'_I)T(x_S) = \sqrt{V_I}\psi^I_0(x'_I) \int_{x_S} \sqrt{g_S}\, G(x_S, x'_S)T(x_S), \tag{4.33}$$

where

$$G(x_S, x'_S) = \sum_m \frac{\psi^S_m(x_S)\psi^S_m(x'_S)}{E_m} \tag{4.34}$$

is the Green's function on the spacetime factor.

If we want to calculate the scalar analog of our double integral eq.(4.11), we can apply eq.(4.34) as long as one of the two scalar sources (which we call T_{min} and T_{probe} in parallel with eq.(4.11)) are constant on the internal space. For concreteness, assume T_{min} is constant. We can now use eq.(4.34) to write (using $\psi^I_0(x'_I) = V_I^{-1/2}$)

$$\begin{aligned} I &\equiv \int_{x_S,x_I,x'_S,x'_I} \sqrt{g}\sqrt{g'}\; T_{min}(x_S)G(x_S, x_I, x'_S, x'_I)T_{probe}(x'_S, x'_I) = \\ &= \int_{x_S,x'_S} \sqrt{g_S}\sqrt{g'_S}\, T_{min}(x_S)G(x_S, x'_S)T^{eff}_{probe}(x'_S), \end{aligned} \tag{4.35}$$

with

$$T^{eff}_{probe}(x'_S) = \int_{x'_I} \sqrt{g_I}\, T_{probe}(x'_S, x'_I). \tag{4.36}$$

That is, I reduces to the analogous double integral in the lower dimensional spacetime with the lower dimensional propagator coupling T_{min} to an effective source T^{eff}_{probe}, which is the integral of T_{probe} over the internal space. If T_{probe} is constant on the internal space as well, the effective source simply picks up a factor of the internal volume.

How much does this structure carry over to the gravitational case of interest for the EE? The gravitational Green's function can still be written in terms of modes. For example in the early work on (anti) de-Sitter space [102, 103] the gravitational Green's function was written as a superposition of eigenmodes of $\mathcal{W}_{\mu\nu}{}^{\lambda\rho}$:

$$G_{\mu\nu\rho\sigma} = \sum_{k=0}^{\infty} a_k h^k_{\mu\nu} h^k_{\rho\sigma} + \sum_{k=1}^{\infty} b_k V^k_{\mu\nu} V^k_{\rho\sigma} + \sum_{k=2}^{\infty} c_k W^k_{\mu\nu} W^k_{\rho\sigma} + \sum_{k=0}^{\infty} d_k \chi^k_{\mu\nu} \chi^k_{\rho\sigma} + \sum_{k=2}^{\infty} e_k [\chi^k_{\mu\nu} W^k_{\rho\sigma} + \leftrightarrow]. \tag{4.37}$$

Here h, V, W, and χ are all orthonormal eigenmodes of $\mathcal{W}_{\mu\nu}{}^{\lambda\rho}$ with different tensor structure: W and V are traceless tensors and correspond to longitudinal and shear tensor modes, h are the genuinely spin-2 transverse traceless modes, and χ are pure trace modes.

In a product spacetime, a similar decomposition of the propagator into eigenmodes with different tensor structures still exists. In particular, one of the terms in the expression for $G_{\mu\nu\rho\sigma}$ will come from gravitational fluctuations with both indices on the "spacetime" part of the product manifold so that the mode is a genuine tensor in spacetime but a scalar in the internal space:

$$G_{\mu\nu\rho\sigma}(x_S, x_I, x'_S, x'_I) = \sum_{n,m} \frac{\psi^{m,S}_{\mu\nu}(x_S)\psi^{m,S}_{\rho\sigma}(x'_S)\psi^I_n(x_I)\psi^I_n(x'_I)}{E_n + E_m} + \dots . \tag{4.38}$$

Here the ψ^I_n are the scalar eigenmodes in the internal space. Clearly for this particular contribution to the propagator, the same simplifications as in the scalar analog integral occur, when we integrate against a source $T^{\mu\nu}_{min}$ that only produces a metric perturbation which is constant on the internal space and only has non-vanishing components with both indices in spacetime. Unfortunately a generic source will give rise to non-vanishing components of *all* modes, including those which are vectors or tensors on the internal space. For the EE however one of our sources, $T^{\mu\nu}_{min}$, is very special in that it is the stress tensor of a codimension-2 minimal surface wrapping the entire internal manifold. It being a minimal

surface implies that

$$T^{\mu\nu}_{min} = \alpha_0 \ \gamma^{ab} X^{\mu}_{,a} X^{\nu}_{,b}, \tag{4.39}$$

where γ^{ab} still denotes the induced metric, α_0 is a constant, and a, b label the worldvolume directions. From eq.(4.39) we see immediately that, for a codimension-2 minimal surface, $T^{\mu}_{\mu} = (D-2)\alpha_0$, where D stands for the total dimension of the product spacetime. The fact that the minimal area wraps the internal space (that is, the minimal area itself is of the form $\mathcal{N} \times I$ where $\mathcal{N}$ is a minimal submanifold of the spacetime factor whereas I is the entire internal space) implies that all internal components of the stress tensor are just α_0 times the spacetime metric; in particular this implies that all mixed spacetime/internal components of $T^{min}_{\mu\nu}$ vanish. Last but not least the fact that the minimal area is codimension-2 also implies that for the trace reversed stress tensor,

$$\tilde{T}_{\mu\nu} = T_{\mu\nu} - \frac{1}{D-2} g_{\mu\nu} T^{\rho}_{\rho}, \tag{4.40}$$

all internal components of $\tilde{T}^{min}_{\mu\nu}$ vanish.

This statement is important, since the trace reversed Einstein equations

$$R_{\mu\nu} = \tilde{T}_{\mu\nu} \tag{4.41}$$

then translate into that the stress tensor of the EE minimal surface does not force any change in the Ricci tensor associated with the internal space, and the unperturbed internal metric solves the full equations of motion. None of the non-trivial tensor or vector modes on the internal space are sourced. For general Freund-Rubin compactifications [104], which includes the $\mathrm{AdS}_5 \times S^5$ background of type IIB supergravity and its $\mathrm{AdS}_{4/7} \times S^{7/4}$ M-theory cousins, this can e.g. be seen explicitly in the work of [105] where the full fluctuation spectrum in such compactifications was determined. A trace reversed stress tensor, with only components on the AdS part turned on, sources only modes which are scalar spherical harmonics on the internal sphere.

So for the case of interest where one of the stress tensors in the double integral of eq.(4.11) is $T^{min}_{\mu\nu}$ with the special properties elucidated above, the double integral can be reduced, just as in the scalar case, to the same double integral performed only over the

spacetime part, with the probe stress tensor replaced by an effective probe brane stress tensor obtained from integrating the full probe stress tensor over the internal space

$$T_{\mu\nu}^{probe,eff} = \int_{x_I} \sqrt{g_I}\, T_{\mu\nu}^{probe}. \tag{4.42}$$

Here μ, ν in eq.(4.42) only run over the spacetime indices of the product manifold. The effective probe stress tensor has no internal components. The full probe stress tensor generically has non-trivial internal components (even in trace reversed form), but as the minimal area did not source any metric perturbation in the internal space, the internal components of the probe stress tensor have nothing to couple to, and do not contribute to the double integral.

For probe stress tensors that are proportional to the metric on the internal space (as one would get if the probe is governed by a DBI action with no fluxes on the internal space turned on), the effective probe stress tensor can be derived from a DBI action solely defined on the spacetime part of the product space, with an effective tension given by the full probe tension times the volume of the internal space. For the D3/D7 and the D3/D5 systems the values of the effective tension (both T_0 and t_0 defined in eq.(4.5)) are

probe	T_0	t_0
D5 on $AdS_4 \times S^2$	$N_f N \frac{\sqrt{\lambda}}{2\pi^3}$	$\frac{N_f}{N}\frac{4\sqrt{\lambda}}{\pi}$
D7 on $AdS_5 \times S^3$	$N_f N \frac{\lambda}{(2\pi)^4}$	$\frac{N_f}{N}\frac{\lambda}{2\pi^2}$

Here we are working in units where the curvature radius of AdS_5 is $L = 1$ and so we have $\alpha'^{-2} = 4\pi g_s N_c = g_{YM}^2 N_c = \lambda$. The 10d Newton's and 5d Newton's constant are given by

$$(16\pi G_{N,10})^{-1} = \frac{4N^2}{(2\pi)^5}, \quad (16\pi G_N)^{-1} = V_5^S (16\pi G_{N,10})^{-1} = \frac{N^2}{8\pi^2} \tag{4.43}$$

respectively, where V_m^S is the volume of the unit m-sphere. The calculation of the EE in the D3/D5 and D3/D7 system now simply boils down to the determination of the EE in the two toy examples of the previous section with these particular values for the tension.

4.5 Taming the UV divergences and Performing the Integrals

4.5.1 Preliminaries

We derived a general prescription for calculating EEs in generic probe brane systems, eq.(4.11). As a confirmation, we now calculate the EE using our formalism in the two solvable toy models (the spacetime filling brane and the codimension-1 RS brane) introduced in section 4.3. We'll compare our answer from the double integral, that is correct to leading order in the backreaction, to the exact expression, which is possible to obtain in these two models as the fully backreacted metric is available in closed form. We also showed in the last section that the leading order answers we calculate in these toy models are, in fact, directly applicable to two of the most interesting top-down systems: the D3/D7 system with the D7 wrapping $AdS_5 \times S^3$ and the D3/D5 system with the D5 wrapping $AdS_4 \times S^2$. For the special case of a spherical entangling surface we also compare our answers to an alternate method based on the trick of [66, 67].

One subtlety we have to deal with is that the double integral eq.(4.11) as it stands is naively doubly UV divergent: both the z-integral over the probe brane worldvolume as well as the w-integral over the minimal area appear UV divergent. We'll deal with these two UV divergences in turn and will calculate the integrals in our two examples. We'll see that the UV divergence in the z-integral is a gauge artifact and can easily be removed. The easiest way to do so is to evaluate the integrals by the not-even-trying method [106]. The UV-divergences in the w-integral on the other hand are physical, and reflect the fact that most contributions to the EE are sensitive to short distance physics. We explicitly regulate the double integral and evaluate all terms in the EE, universal and cut-off dependent ones. In order to isolate the contributions due to the probe brane, we subtract off the EE of the field theory without the probe.

4.5.2 The probe brane z integral

While the double integral for the EE is symmetric between probe and minimal area, from the physical point of view it is most natural to first perform the z integral to obtain the backreacted metric, and then to do the w integral next in order to evaluate the resulting

change in the EE. To do so, we need to first specify the propagator: both of our examples calculate the probe EE in a background AdS space; furthermore, the examples we consider all involve both a static probe brane and a static minimal area. So there is no time dependence involved and we can use the Euclidean AdS graviton propagator of [84]:

$$\begin{aligned} G_{\mu\nu\mu'\nu'}(w-z) &= (\partial_\mu\partial_{\mu'}u\partial_\nu\partial_{\nu'}u + \partial_\mu\partial_{\nu'}u\partial_\nu\partial_{\mu'}u)G(u) + g_{\mu\nu}g_{\mu'\nu'}H(u) \\ &\quad +(\partial_{(\mu}[\partial_{\nu)}\partial_{\mu'}u\partial_{\nu'}uX(u)] + (\partial_{(\mu'}[\partial_{\nu')}\partial_\mu u\partial_\nu uX(u)] \\ &\quad +(\partial_{(\mu}[\partial_{\nu)}u\partial_{\mu'}u\partial_{\nu'}uY(u)] + (\partial_{(\mu'}[\partial_{\nu')}u\partial_\mu u\partial_\nu uY(u)] \\ &\quad +\partial_\mu[\partial_\nu Z(u)]g_{\mu'\nu'} + \partial_{\mu'}[\partial_{\nu'}Z(u)]g_{\mu\nu}. \end{aligned} \tag{4.44}$$

Here u is the geodesic distance,

$$u \equiv \frac{(z-w)^2}{2z_0w_0} = \frac{(\vec{z}-\vec{w})^2 + (z_0-w_0)^2}{2z_0w_0}, \tag{4.45}$$

primed (unprimed) derivatives are derivatives with respect to z (w), and $(\cdots)$ denotes symmetrization with unit strength. The advantage of writing the propagator in this form is that it is manifestly engineered to isolate the gauge invariant information: the terms involving X, Y and Z are gradients with respect to w or z. These w gradient terms correspond to a gauge transformation we perform on the resulting $(\delta g)_{\mu\nu}(w)$ we get from integrating the propagator against $T^{probe}_{\mu'\nu'}(z)$. The w gradients are annihilated by the differential operator $\mathcal{W}_{\mu\nu}{}^{\lambda\rho}$ from eq.(4.27) - Einstein's equations only determine the metric up to a gauge transformation. The gradients with respect to z can be absorbed into the gauge transformation parameter $\Lambda_{\mu\nu\nu'}$ appearing on the right hand side of the defining differential equation for $\mathcal{W}_{\mu\nu}{}^{\lambda\rho}$, eq.(4.26). When contracted against conserved stress tensors, these total derivative terms can be integrated by parts and do not contribute as long as the sources vanish at infinity. The full gauge invariant information in the propagator is contained in the functions $G(u)$ and $H(u)$ which were determined in [84].

Unfortunately this beautiful formalism fails to give a finite answer for sources that extend to the boundary, as is the case for most probe brane systems of interest. Close to the boundary, $u \to \infty$, G and H vanish as $G \sim u^{-d}$ and $H \sim u^{2-d}$. Taking into account the tensor structure in the propagator, for both terms the leading behavior near the boundary is u^{4-d}; taking the measure into account the integrand goes as u^4. Hence the source $T^{\mu\nu}_{probe}$

has to vanish faster than u^4 for the integral to remain finite. For a $T^{\mu\nu}_{probe}$ corresponding to a finite energy density this is the case. For a probe brane extending to infinity, where the non-vanishing components of $T^{\mu\nu}_{probe}$ typically go as $g^{\mu\nu} \sim u^{-2}$, the integral diverges as u^2. Since H and G multiply different tensor structures these divergences do not cancel against each other. What keeps the integral finite in the end are the "gauge variant" terms in the propagator, X, Y and Z. When integrated against the non-vanishing $T^{\mu\nu}_{probe}$ they leave divergent boundary terms behind which have to cancel the divergences due to G and H. Unfortunately this means one needs to know the full propagator and not just G and H.

Fortunately the same authors in [106] put forward an alternative method to do z-integrals without-even-trying which automatically cures these UV divergences. Instead of calculating the integral directly, one applies $\mathcal{W}_{\mu\nu}{}^{\lambda\rho}$ on the integral

$$(\delta g)_{\mu\nu} = \int (d^{n+1}z\sqrt{g_I}) G_{\mu\nu\mu'\nu'} T^{\mu'\nu'}_{probe} \tag{4.46}$$

and, using eq.(4.26), derives a simple differential equation for the integral itself. The astute reader will notice that this method essentially boils down to abandoning the Green's function approach and simply solving linearized Einstein's equations directly. There are however still advantages in thinking about the integral. For highly symmetric situations, as the one considered here, the inversion properties of the integral can be used to argue that the resulting metric deformation can only depend on a single variable, rendering Einstein's equations to be linear ODEs. Equivalence between the not-even-trying method with the direct evaluation of the integral was explicitly confirmed in [106]. So, to do the integral, we can study the simpler problem of solving linearized Einstein's equations directly. The upshot is that the result of the z integral are the metric perturbations eq.(4.16) and eq.(4.25) for the codimension-0 and codimension-1 branes in AdS_{d+1} respectively.

To be a little bit more precise let us quickly work through the codimension-1 case. Let w_0 denote the radial direction as before, w_1 the spatial direction orthogonal to the defect and $\mathbf{w}$ the spatial directions along the defect. Rotation and translation invariance in $\mathbf{w}$ directions tell us the δg can not depend on $\mathbf{w}$ and that the only allowed tensor structures in δg are

$$(\delta g)_{\mu\nu} = f_1\, g_{\mu\nu} + f_2\, (P_0)_\mu (P_0)_\nu + f_3\, (P_1)_\mu (P_1)_\nu + f_4\, [(P_1)_\mu (P_0)_\mu + (P_0)_\nu (P_1)_\mu]. \tag{4.47}$$

Here $(P_{0/1})_\mu$ are simply the projectors $\delta_\mu^{0/1}/w_0$. In principle the functions f_1 through f_4 can depend on w_0 and w_1, but by invariance of the integral under scaling of w_0 and w_1, we can see that in fact they can only depend on $t = w_0/w_1$. Acting on $(\delta g)_{\mu\nu}$ with $\mathcal{W}_{\mu\nu}{}^{\lambda\rho}$ one derives a simple set of ODEs for f_1 through f_4 as a function of t with the probe brane stress tensor evaluated at w appearing as the source. Naively this set of differential equations looks over-determined, but it is easy to confirm that our δg of eq.(4.25) indeed satisfies all of them as expected. The same method should still work if we include extra terms in the brane stress tensor, for example an electric field in the radial direction.

4.5.3 The minimal area w integral

The w integral is also UV divergent. Unlike the UV divergences in the z integral, the UV divergencies in the w integral are physical and reflect the short distance sensitivities of the EE. As long as the entangling surface intersects with the conformal defect, there exists a UV divergence in the probe contribution to the EE due to the entanglement from those short-distance degrees of freedom of the defect theory. They manifest themselves via the standard EE divergent structure of the conformal defect-localized sector. So in order to do the w integral and to isolate and calculate these UV sensitive terms as well as the universal remainders, we need to chose a regularization procedure. This turns out to be an essential but subtle step.

In order to isolate the EE due to the probe, we need to ensure that we do not modify the contribution from the non-probe degrees of freedom, dual to bulk gravity. It turns out, following [82], that we need to modify the holographic renormalization procedure for the leading contribution to the EE in order to ensure that this is the case. Due to the backreaction of the probe brane, the induced metric on the original cutoff slice will be slightly altered, and so will the leading order EE associated with the non-probe degrees of freedom. In order to avoid this effect we need to chose a new cut-off surface, constructed so that the induced metric on the cutoff slice is the same in the perturbed metric with the new cutoff as it was in the unperturbed metric with the old cutoff. Formally we can write

$$\delta A = \left(A\left[g'\right]_{\Sigma'} - A\left[g\right]_{\Sigma}\right)_{\gamma_{\Sigma'}[g']=\gamma_\Sigma[g],} \tag{4.48}$$

with $A[g]_\Sigma$ being the area of the minimal surface calculated with the given metric g and cutoff slice Σ, and $\gamma_\Sigma[g]$ being the induced metric of g onto Σ. In particular, the constraining relation above can be solved, providing the explicit definition of the new cutoff slice, $\Sigma' = \Sigma'(g'; g, \Sigma)$, constructed in such a way that the induced metric for the boundary is the same for both g on Σ and g' on Σ'. Therefore, the backreaction from the probe-brane perturbation enters the final result not only as the change of the integrand through metric perturbation, but also as the change of integration domain from a new UV cut-off slice associated with the perturbation. In our formal expressions for the variation of the area as response to a metric perturbation, this effect was not visible, as it is all about regulating the UV divergences.

While in general this change of UV cutoff seems to be rather complicated, in the probe brane limit we are working with, these two contributions disentangle nicely from each other to the leading order of probe brane tension. We can write such disentangling effect formally as:

$$\delta A = \left(A\left[g+\delta g\right]_\Sigma - A\left[g\right]_\Sigma\right) + \left(A\left[g\right]_{\Sigma'(g';g,\Sigma)} - A\left[g\right]_\Sigma\right) + O\left(t_0^2\right). \tag{4.49}$$

That is, to correctly capture the effects to leading order in t_0, we need to calculate the change in area due to the perturbed metric with the old cutoff, as well as the change in the original area due to the new cutoff. We can neglect the contribution from integrating the change in the area from the old to the new cutoff, as that term is order t_0^2.

The first regularized term allows the canonical treatment of the variational principle with Dirichlet boundary condition, and our double integral formula applies straightforwardly. The second subtraction term is constructed according to the principle of using the same holographic renormalization scheme before and after perturbation. It admits a simple geometrical interpretation as the difference of the minimal surface bounded between the original cutoff plane and the associated new cutoff plane. In what follows we will see that it is crucial to include this extra contribution in order to get sensible answers for the probe EE.

The codimension-1 RS brane and the D3/D5 system

As a first consistency check of our procedure, we want to calculate the EE for the codimension-1 RS brane and compare it to the exact answer obtained from the fully backreacted metric. In addition, for this case of a conformal probe brane in a conformal background, an alternative method exists to get the EE. As recently pointed out by Jensen and O'Bannon, in this case one can apply the trick of [67] to determine the EE by mapping it to a thermal entropy in a hyperbolic space. We review the Jensen-O'Bannon calculation in Section 4.6. Reassuringly, we will find that all three calculations agree.

In order to apply our tools for the probe calculation, we first need to determine the correct UV cutoff on the w integral. For the EE calculation in the unperturbed AdS_{d+1} background one typically chooses the flat cutoff plane $w_0^* = \epsilon$ in the AdS Poincaré coordinates. To calculate the associated cutoff surface due to the perturbation in the toy model, it is much easier to work with the perturbation in the original AdS-sliced coordinates as in eq.(4.19):

$$ds^2 = dr^2 + \frac{\cosh^2(|r| - c)}{y^2}(dy^2 + dt^2 + d\vec{w}^2) \to dr^2 + \frac{\cosh^2 r - 2c\cosh r \ \sinh|r|}{y^2}(dy^2 + dt^2 + d\vec{w}^2), \tag{4.50}$$

with AdS-radius L scaled to 1. In this coordinate system the original UV cut-off plane is located at $w_0^* = \frac{y}{\cosh r} = \epsilon$. The perturbation-corrected cutoff surface is given by the following locus:

$$\cosh r = \frac{y}{\epsilon}(1 + c\frac{\sqrt{y^2 - \epsilon^2}}{y}). \tag{4.51}$$

With this subtraction scheme we present two cases for this toy model: a spherical entangling surface bisected by the defect, and a strip entangling surface containing the defect.

Case 1 - Spherical Entangling Surface: Choosing the spherical entangling surface bisected by the defect, the minimal surface in AdS_{d+1} turns out to be [68] the $d-1$ dimensional hemisphere

$$R^2 = w_0^2 + w_1^2 + \vec{w}^2 = y^2 + \vec{w}^2. \tag{4.52}$$

Using the AdS-sliced coordinate, the induced metric on the minimal area and its stress

tensor are given by:

$$\sqrt{\gamma} = \left(\frac{\cosh r}{y}\right)^{d-2} (1-y^2)^{\frac{d-4}{2}}\, vol^S_{d-3}, \tag{4.53}$$

$$\frac{1}{2}\gamma^{ab} x^\mu_{,a} x^\nu_{,b} \delta g_{\mu\nu} = -c \tanh r * Tr[\mathbb{1}_{(d-2)}] = -c\,(d-2)\tanh r, \tag{4.54}$$

where vol^S_m denotes the volume form of the unit m-sphere.

To calculate the EE we need to calculate the change in area from our double integral formula eq.(4.11), and then subtract from it the contribution from the change of cutoff as indicated in eq.(4.49). Using the metric perturbation eq.(4.22) we have from the double integral (using $c_r \equiv \cosh r$ as an integration variable)

$$I_1 = \frac{1}{4G_N} V^S_{d-3}\, 2 \int_\epsilon^1 dy \int_1^{\frac{y}{\epsilon}} dc_r\, [-c(d-2)c_r^{d-3}] \frac{(1-y^2)^{\frac{d-4}{2}}}{y^{d-2}}. \tag{4.55}$$

The factor of 2 comes about since we need to integrate from the midpoint ($c_r = 1$) both to positive and negative infinity in r. By symmetry this is twice the integral to large positive r. The original minimal area integrated from old and new cutoff gives us

$$I_2 = \frac{1}{4G_N} V^S_{d-3}\, 2 \int_\epsilon^1 dy \int_{\frac{y}{\epsilon}}^{\frac{y}{\epsilon}(1+c\sqrt{1-\frac{\epsilon^2}{y^2}})} dc_r\, \frac{c_r^{d-2}}{\sqrt{c_r^2-1}} \frac{(1-y^2)^{\frac{d-4}{2}}}{y^{d-2}}. \tag{4.56}$$

Note that the y-integral is already the same in both I_1 and I_2, but the c_r integrals differ. Looking at the sum of I_1 and I_2 we see that the c_r integral we need to do is

$$\tilde{I} \equiv -c(d-2)\int_1^{\frac{y}{\epsilon}} dc_r\, c_r^{d-3} + \int_{\frac{y}{\epsilon}}^{\frac{y}{\epsilon}(1+c\sqrt{1-\frac{\epsilon^2}{y^2}})} dc_r\, \frac{c_r^{d-2}}{\sqrt{c_r^2-1}}. \tag{4.57}$$

As we are only interested in the leading $c \sim t_0$ behavior, we can expand out the second term in a power series in c,

$$\int_{\frac{y}{\epsilon}}^{\frac{y}{\epsilon}(1+c\sqrt{1-\frac{\epsilon^2}{y^2}})} dc_r\, \frac{c_r^{d-2}}{\sqrt{c_r^2-1}} = c\left(\frac{y}{\epsilon}\right)^{d-2} + \mathcal{O}(c^2), \tag{4.58}$$

so that we simply get $\tilde{I} = c + \mathcal{O}(c^2)$. The probe contribution to the EE then becomes

$$S_A = \frac{1}{2G_N} V^S_{d-3} c \int_\epsilon^1 dy\, \frac{(1-y^2)^{\frac{d-4}{2}}}{y^{d-2}} = \frac{2\pi T_0}{d-1} V^H_{d-2}. \tag{4.59}$$

Here we used eq.(4.5) and eq.(4.21) (with the radius of curvature set to 1) to re-express c in terms of T_0 and recognized the y integral as the (regulated) volume of the unit hyperboloid

as defined in Section 4.6. As also reviewed there, V^H_{d-2} is exactly the structure to expect from a conformal field theory is $d-1$ dimensions; the EE for the defect degrees of freedom has the same functional form as that of a CFT living on the defect.

This answer is in perfect agreement with the Jensen-O'Bannon result of Appendix A. It is also in perfect agreement with the answer we get in the fully backreacted solution as we will now show. In the fully backreacted solution, the minimal area is locally given by the same embedding, so the worldvolume area element is still given by $\cosh^{d-2}\bar{r}$ where $\bar{r} = r - c$ for $r > 0$. To isolate the EE contribution due to the defect, we still need to subtract out the EE for the theory without the defect. Matching cutoff procedures requires that we truncate both integrals at the same value of the warpfactor, $\cosh\bar{r}_* = \cosh r_*$. Since the r integral starts at 0, whereas the $\bar{r}$ integral starts at $-c$, the difference is given by a $\bar{c}_r$ integral between these finite values. As y no longer appears as an integration boundary, the two integrals factorize and the defect EE is given by

$$S_A = \frac{1}{2G_N} V^S_{d-3} \int_0^{-coshc} d\bar{c}_r \, \frac{\bar{c}_r^{d-2}}{\sqrt{\bar{c}_r^2 - 1}} \int_\epsilon^1 dy \, \frac{(1-y^2)^{\frac{d-4}{2}}}{y^{d-2}} = \frac{1}{2G_N} F(c)\, V^H_{d-2}. \tag{4.60}$$

Here

$$F(c) = \int_0^{\cosh c} dc_r \frac{c_r^{d-2}}{\sqrt{1-c_r^2}} \tag{4.61}$$

is a non-linear function of $c = \tanh^{-1}(4\pi G_N T_0/(d-1))$ that can easily be evaluated in terms of hypergeometric functions. What is important here is that, in the limit of small c, we have

$$F(c) = c + \mathcal{O}(c^2) \tag{4.62}$$

which can e.g. easily be seen by changing variables from c_r to x, where $c_r = 1 + x^2/2$ and expanding the integral for small x. Plugging in $c \sim 4\pi G_N T_0/(d-1)$ for small c, we see that the fully backreacted EE of eq.(4.60) indeed reduces to the probe limit answer of eq.(4.59) when linearizing the full answer in the brane tension.

Case 2 - Strip Entangling Surface: Choosing the static gauge for strip entangling surface along the x^1-direction in the Poincaré patch as eq.(4.13), $U^{d-1} = \{(w^0, \vec{w})\} \hookrightarrow AdS_{d+1}$, one can verify that the minimal surface is given by solving the following equation: x^d

being any constant (the specific time for the entangling surface), $x^0 = w^0$, $x^{i+1} = w^i$ for $i \in \{1, 2, \ldots, d-2\}$, and

$$\frac{dx^1}{dw^0} = \frac{\pm 1}{\sqrt{\left(\frac{L_U}{w^0}\right)^{2d-2} - 1}}. \tag{4.63}$$

Using translational and scaling transformations, we can place the strip in the following 2-branched parametrization located around the origin,

$$x^1 = \pm L_U \left(\frac{1}{d} \left(\frac{w^0}{L_U} \right)^d {}_2F_1 \left[\frac{1}{2}, \frac{d}{2d-2}, \frac{3d-2}{2d-2}, \left(\frac{w^0}{L_U} \right)^{2d-2} \right] \mp \frac{\sqrt{\pi}}{d} \frac{\Gamma\left[\frac{3d-2}{2d-2}\right]}{\Gamma\left[\frac{2d-1}{2d-2}\right]} \right), \tag{4.64}$$

with L_U being its endpoint in the radial x^0-coordinate, $\mp \frac{L_U \sqrt{\pi}}{d} \frac{\Gamma\left[\frac{3d-2}{2d-2}\right]}{\Gamma\left[\frac{2d-1}{2d-2}\right]}$ being its two endpoints in the perpendicular x^1-direction to the defect on the boundary. For applying our formula eq.(4.11), we first notice that,

$$\sqrt{\gamma} = \frac{L^{d-1}}{(w^0)^{d-1}\sqrt{1 - \left(\frac{w^0}{L_U}\right)^{2d-2}}} \to \frac{1}{(w^0)^{d-2}\sqrt{(w^0)^2 - (w^0)^{2d}}}, \tag{4.65}$$

where we temporarily restore the factor of AdS-radius L, given another length scale, strip-depth L_U, is also present, in order to correctly identify the scaling forms of both factors. With this, we can then safely rescale the w^0-coordinate from 0 to 1 for the further evaluation. The rest of integrand, $\gamma^{ab} x^\mu_{,a} x^\nu_{,b} \delta g_{\mu\nu}$ (the $\frac{1}{2}$ is canceled due to the identical contribution from the two branches), can be obtained by noticing that the metric perturbation eq.(4.25) separates into two independent sectors of $x^{(0,1)}$-subspace and $\vec{x}$-subspace: For the $x^{(0,1)}$-subspace, given the metric perturbation is also in the form of direct product, $\delta g_{\mu\nu} = \frac{-2\tilde{c}|x^1|}{(x^0)^2\sqrt{(x^0)^2+(x^1)^2}} u_\mu u_\nu$ with $u_\mu = \frac{(x^0, x^1)}{\sqrt{(x^0)^2+(x^1)^2}}$ and $\tilde{c} = \frac{t_0}{4(d-1)}$, we immediately have:

$$\left(\gamma^{ab} x^\mu_{,a} x^\nu_{,b} \delta g_{\mu\nu}\right)_{x^{(0,1)}\text{-subspace}} = \gamma^{00} \frac{-2\tilde{c}|x^1|}{(x^0)^2\sqrt{(x^0)^2 + (x^1)^2}} (x^\mu_{,0} u_\mu)(x^\nu_{,0} u_\nu), \tag{4.66}$$

with

$$\gamma_{00} = \frac{1 + \left((x^1)'\right)^2}{(w^0)^2} \to \gamma^{00} = (w^0)^2 \left(1 - (w^0)^{2d-2}\right), \tag{4.67}$$

and

$$x^\mu_{,0} u_\mu \to \frac{1}{(w^0)^2 + (x^1)^2} \left(w^0 + \frac{x^1 (w^0)^d}{\sqrt{(w^0)^2 - (w^0)^{2d}}} \right). \tag{4.68}$$

Consequently, we have

$$\left(\gamma^{ab}x^{\mu}_{,a}x^{\nu}_{,b}\delta g_{\mu\nu}\right)_{x^{(0,1)}\text{-subspace}} \to \frac{-2\tilde{c}|x^1|}{\sqrt{(w^0)^2+(x^1)^2}}\frac{\left(1-(w^0)^{2d-2}\right)}{(w^0)^2+(x^1)^2}\left(w^0+\frac{x^1(w^0)^d}{\sqrt{(w^0)^2-(w^0)^{2d}}}\right)^2. \tag{4.69}$$

For the $\vec{x}$-subspace, given the metric perturbation eq.(4.25) equals to the original AdS_{d+1} metric with an extra scaling factor $\frac{-2\tilde{c}|x^1|}{\sqrt{(x^0)^2+(x^1)^2}}$, the result is

$$\left(\gamma^{ab}x^{\mu}_{,a}x^{\nu}_{,b}\delta g_{\mu\nu}\right)_{\vec{x}\text{-subspace}} \to \frac{-2\tilde{c}|x^1|}{\sqrt{(x^0)^2+(x^1)^2}}\text{Tr}[\mathbb{1}_{d-2}] = \frac{-2\tilde{c}|x^1|}{\sqrt{(x^0)^2+(x^1)^2}}(d-2). \tag{4.70}$$

Given eq.(4.65),(4.69),(4.70), the final result for the strip entanglement entropy density, after we factor out the translational invariant subspace spanned by $\vec{w}$, with the constant cutoff slice $w^0=\epsilon$, is given by

$$\int_{\epsilon}^{1}\frac{dw^0}{(w^0)^{d-2}\sqrt{(w^0)^2-(w^0)^{2d}}}\frac{(-2\tilde{c}|x^1|)\left(d-2+\frac{(w^0)^2-(w^0)^{2d}}{(x^1)^2+(w^0)^2}\left(1+\frac{x^1(w^0)^{d-1}}{\sqrt{(w^0)^2-(w^0)^{2d}}}\right)^2\right)}{\sqrt{(x^1)^2+(w^0)^2}}, \tag{4.71}$$

together with the cutoff effect, eq.(4.49), which after some algebra can be rewritten succinctly into the following compact subtraction term:

$$\frac{S_{sub}}{\text{Vol}^{d-2}_{Span\{\vec{w}\}}} = \left(\frac{2\tilde{c}x^1}{\sqrt{(x^1)^2+(w^0)^2}}\frac{1}{(w^0)^{d-2}}\right)_{w^0\to\epsilon}, \tag{4.72}$$

with $\text{Vol}^{d-2}_{Span\{\vec{w}\}}$ being the volume of translational invariant $d-2$ dimensional subspace spanned by $\vec{w}$, x^1 being the minimal embedding function eq.(4.64) rescaled by $L_U\to 1$. The change of minimal surface area density, according to eq.(4.49), will be given by the difference of eq.(4.71) and eq.(4.72).

Even though the above expressions seem daunting, simple numerical investigation nevertheless reveals that the difference numerically evaluates to $2.0c$ for AdS_4 up to AdS_7, before numerical instabilities render the evaluation inconclusive. After restoring the relevant scales, this change of entanglement entropy density can be expressed as:

$$s_A = \frac{S_A}{\text{Vol}^{d-2}_{Span\{\vec{w}\}}} = \frac{1}{4G_N}\left(2.0\ \tilde{c}\ \frac{L^{d-1}}{L_U^{d-2}}\right) = \frac{2.0\pi T_0}{(d-1)}\frac{L^d}{L_U^{d-2}},\ \text{for } d\in\{4,5,6,7\}, \tag{4.73}$$

with $\tilde{c}$ being re-expressed in terms of T_0 using eq.(4.5) and eq.(4.21). Notice that this constant result also coincides with the result for AdS_3 obtained by [82]. It is very tempting to conjecture that this numerical result also holds for any higher dimension. It should be possible to verify this simple answer analytically, but we will not pursue it further.

Note that in this case the answer for the defect contribution to the EE was UV finite. This is not too surprising, as the entangling surface did not intersect the defect and so there is no short range entanglement.

The spacetime filling probe and the D3/D7 system

Let us next calculate the EE for the spacetime filling probe brane, using our double integral prescription and once more compare it both to the exact answer from the fully backreacted metric as well as the Jensen-O'Bannon analysis from Section 4.6. The EE in this case is straight forward to calculate, as the bulk spacetime remains AdS_{d+1} just with a shifted curvature radius given by eq.(4.15). In order to see the consequences of this shift in L, let us restore the curvature radius in the expression for the EE for a spherical entangling surface of radius R using an AdS_{d+1} with curvature radius L [107]:

$$S_A = \frac{L^{d-1}}{4G_N} V^S_{d-2} \int_{R/a}^{1} dy \, \frac{(1-y^2)^{(d-3)/2}}{y^{d-1}} = \frac{L^{d-1}}{4G_N} V^H_{d-1}. \tag{4.74}$$

We see that the sphere radius only enters into the definition of ϵ in the regulated V^H. The overall L^{d-1} factor cancels the dimensions in Newton's constant. Simply replacing L with l according to eq.(4.15) we see that the fully backreacted contribution to the EE by the spacetime filling brane is (setting $L = 1$ in the final answer to compare with expressions elsewhere in this paper)

$$S_A = \frac{l^{d-1} - L^{d-1}}{4G_N} V^H_{d-1} = \frac{2\pi T_0}{d} V^H_{d-1} + \mathcal{O}(t_0^2) \tag{4.75}$$

in complete agreement with the Jensen-O'Bannon formula from Section 4.6.

To reproduce this calculation from our double integral formula, we once more need to add up two contributions. For one we have the direct contribution from the double integral,

regulated by the old cutoff at[6] $z/L = \epsilon$. In addition, we argued above that one should include a contribution from the changed cutoff, which is the integral of the original action from the old to the new cutoff. Matching cutoffs requires that $L/\epsilon = l/\epsilon$, so that the short distance cutoff a, which actually sets the range of our integrals, remains unchanged. Therefore, in the case of the codimension-0 brane, this second contribution vanishes. Since δg is AdS_{d+1} with curvature radius $(\delta L)^2 = t_0 L^2/[d(d-1)]$, we have $T^{\mu\nu}_{min}\delta g_{\mu\nu}/2 = (d-1)/2$ and the double integral is in form identical to the original minimal area integral, just with a different prefactor and we obtain (again setting $L = 1$ in the final answer)

$$S_A = \frac{V^H_{d-1}}{4G_N}\frac{t_0}{2d} = 2\pi T_0 V^H_{d-1}, \tag{4.76}$$

in perfect agreement with both the full non-linear formula and the Jensen-O'Bannon result.

4.6 Comparison with The Jensen-O'Bannon Calculation

Jensen and O'Bannon [66] pointed out that, for the special case of spherical entangling surfaces in a conformal theory where the probe preserves at least a lower dimensional subgroup of the conformal group (such as the D3/D5 and the D3/D7 system studied in the bulk of our paper at least in the absence of mass terms for the fundamental flavors), one can give an alternative derivation of the probe EE using the method of reference [67]. There it was pointed out that in a CFT the EE for a spherical entangling surface can be mapped to the thermal entropy associated with the same theory but formulated on a hyperboloid. The radius of the sphere and the hyperboloid are equal, and as in a CFT this radius sets the only scale, we will work with the unit sphere/unit hyperboloid. The radius of the sphere can be restored by dimensional analysis in the end. In the bulk this conformal transformation can easily be implemented by a change of coordinates. As long as we define the boundary metric by stripping off the quadratic divergence of the metric in the radial direction when approaching the boundary, different radial coordinates are associated with conformally related boundary metrics. AdS_{d+1} can be written in a hyperbolic slicing as

$$ds^2 = -h(r)dt^2 + \frac{dr^2}{h(r)} + r^2 dH^2_{d-1}, \tag{4.77}$$

[6] We require the short distance cut-off length $a = L\epsilon$ to have units of length for dimensionless ϵ, this forces the factor of L into this formula. Also, z/L is the correct warpfactor.

where dH^2 is the metric on the unit hyperboloid, which we can take to be given by

$$dH_{d-1}^2 = d\rho^2 + \sinh^2(\rho)\, d\Omega_{d-2}^2. \tag{4.78}$$

AdS without a black hole corresponds to $h(r) = -1 + r^2/L^2$. While this is the vacuum solution of Einstein's equations, in this coordinate system we see a horizon at $r = L$ with a temperature of $T = (2\pi L)^{-1}$, see [108, 109, 110, 111]. The associated thermal entropy is the EE for the conformally related spherical entangling surface. The thermal entropy of the hyperbolic horizon can be expressed as a finite entropy density (which characterizes the number of degrees of freedom in the dual field theory) times the volume of the hyperboloid. Latter is of course infinite, but can be regulated by introducing a cutoff. In terms of $y = (\cosh\rho)^{-1}$, we can define the volume of the m dimensional unit hyperboloid as the volume contained in the $y \geq \epsilon$ part of the hyperboloid

$$\begin{aligned} V_m^H &= V_{m-1}^S \int_\epsilon^1 dy\, \frac{(1-y^2)^{(m-2)/2}}{y^m} && (4.79) \\ &= p_1 \left(\frac{1}{\epsilon}\right)^{m-1} + p_3 \left(\frac{1}{\epsilon}\right)^{m-3} + \dots \\ &\quad \dots + \begin{cases} p_{m-1}\left(\frac{1}{\epsilon}\right) + p_m + \mathcal{O}(\epsilon) & m \text{ even} \\ p_{m-2}\left(\frac{1}{\epsilon}\right) + q\log(\epsilon) + \mathcal{O}(1) & m \text{ odd.} \end{cases} && (4.80) \end{aligned}$$

Recall that V_m^S denotes the volume of the unit m-sphere. The coefficients p_i can easily be determined from the integral expression. They are spelled out explicitly in [107].

The free energy density of AdS in hyperbolic coordinates is given by the gravitational on-shell action, which in turn simply is the volume of space time

$$\Omega = C_0 \int \sqrt{g} + \mathcal{L}_{ct} = C_0 \int_{r_h=L}^{\Lambda} r^{d-1} + \mathcal{L}_{ct}, \tag{4.81}$$

with $C_0 = d/(8\pi G_N)$. As usual, this expression is divergent and can be regulated by counterterms as we indicated. In fact, in order to systematically treat the d dimensional case it was found to be easier to work with background subtraction, where here the correct background is the zero temperature hyperbolic black hole, which corresponds to a black hole with a negative mass parameter in hyperbolic slicing [108, 109, 110, 111]. In these papers it was explicitly confirmed that in low dimensions the regulation by counterterms is

equivalent to using background subtraction. The corresponding entropy density was found to be (in units of the radius of the hyperboloid)

$$s = \frac{2\pi C_0}{d}. \tag{4.82}$$

As expected, this is just the standard Bekenstein-Hawking entropy, $1/(4G_N)$ times the horizon area.

As the EE for a spherical entangling surface of unit radius is equal to this thermal entropy, it can easily be expressed in terms of V_m^H. Restoring the radius of the sphere, one finds for the EE associated with a sphere of radius R [107]:

$$S = \frac{V_{d-1}^H}{4G_N}, \tag{4.83}$$

where the relation between G_N and field theory quantities depends on the theory in question and the ϵ's appearing in V^H should be read as R/a where a is the short distance cutoff length.

The probe branes of interest for us extend along a minimal AdS_{n+1} slice inside AdS_{d+1}. In the original flat slicing, these minimal AdS_{n+1} branes are obtained by setting some of the spatial components of w_μ to zero. In the hyperbolic coordinates, they are wrapping an equatorial S^{n-2} inside the S^{d-2} in eq.(4.78). The worldvolume action is just the volume of the probe brane, so the free energy density is once more given by the regulated volume. For $n = d$ the calculation proceeds as above and we get

$$S = \frac{2\pi T_0}{d} V_{d-1}^H. \tag{4.84}$$

T_0 here is the effective tension, which for probe branes wrapping a product manifold is the full brane tension times the volume of the internal space, just as we found to be the case more generally in section 4.4. For $n < d$ we also calculate the volume. But one should note that for the background subtraction we are still using the $d+1$ dimensional zero temperature hyperbolic black hole. It's easy to see that for $n < d$ background subtraction simply cancels the UV divergent terms without leaving a finite remainder and the free energy is given by $-T_0 r_h^{n-1}$. To get the entropy density from this, one needs the relation between T and r_h, which for a hyperbolic black hole at $T = (2\pi L)^{-1}$ is given by $r_H = 2\pi T/(d-1)$, instead of

the familiar $r_H = 4\pi T/d$ from flat slicing black holes. With this we get for the entropy for $n < d$:

$$S = \frac{2\pi T_0}{d-1} V_{n-1}^H. \tag{4.85}$$

That is, the EE is equivalent to that of a spherical entangling surface in a $n+1$ dimensional field theory, with the degrees of freedom counted by $(2\pi T_0)/(d-1)$ instead of $1/(4G_N)$.

4.7 Conclusion

In this work we determined the EE for a generic probe brane system as a formal double integral by explicitly taking into account the leading order backreaction of the brane. We validated our formula by working out the EE in various examples, comparing to established answers where possible.

It is somewhat surprising that in order to calculate the EE for a probe brane we actually seem to need to calculate at least the leading order backreaction. This has to be contrasted with calculations of the thermal entropy density, for which knowledge of the on-shell action of the probe itself is completely sufficient. As explained e.g. in [53] the thermal entropy can be obtained using thermodynamic identities from the free energy. Latter can be obtained from the probe action alone. The bulk equations of motion ensure that the leading order backreaction, which naively comes in at the same order as the probe on-shell action, in fact does not contribute to the on-shell action. A direct calculation of the thermal entropy would also involve calculating the backreaction of the probe. Very similar to our calculation here, one would have to calculate the change in the horizon area due to the backreaction. In fact, as horizons are minimal area surfaces in the Euclidean black hole geometry, our formula directly applies to this case as well. As the horizon does typically not extend to the boundary, we even avoid the issues of UV divergences in the w-integral in that case.

By analogy one may hope that, at least in some circumstances, our double integral from eq.(4.11) should simplify to an expression that localizes on the probe worldvolume alone. This is known to be true for the special case of a spherical entangling surfaces for conformal defects, as we made use of at various points in this work. There the calculation directly maps to a thermal entropy calculation and so it can once more be obtained via the free

energy. The simple answer we get for the EE of a strip suggests that this, too, should follow from an easier calculation. The recent derivation of the RT prescription of [112] hints that such a simplification should be possible more generally at least in static backgrounds. It would be interesting to make this more precise.

There are many potential future applications of our method. In this work we only looked at the simplest and most symmetric examples, both for the entangling surface and the probe embedding. More general entangling surfaces are straight forward. Recently the general terms appearing in the EE for boundary and hence also defect CFTs has been worked out (for $d = 4$) in [113]. Our results are in complete agreement with the structure found there, but trivially so. It would be interesting to confirm that the EE for more general entangling surfaces confirms the results of [113]. Maybe more interestingly, our formula should be applied to some of the more interesting probe brane systems described in the introduction, where the EE can hopefully serve as a new probe to disentangle the interesting physics described by these probe branes. In particular, the finite density systems with a non-trivial worldvolume F_{rt} should be easily within reach.

Our results can also be applied to gravitational theories including higher curvature corrections. In this case, it has been argued that the EE should be given by an appropriate Wald-like entropy [114] associated with the minimal area [112, 115], even though it is not the standard Wald entropy. As long as the EE can be written as an integral of a local Lagrangian density over a bulk surface, our formulism will still apply with $T^{min}_{\mu\nu}$ being the stress tensor associated with the new action. Of course higher derivative corrections are then also expected in the probe brane action, for which we allowed a general form already anyway.

Chapter 5

FINAL WORDS

In this thesis, we present our works towards better understandings of the strongly coupled many-body systems with extra fundamental-representation matter content in the quenched limit, using the toolkits from holography via a probe brane construction. The unifying theme of these works is to better understand the novel quantum phases realized using holography. Specifically, for the defect conformal systems, we unearth and quantify the phase trasition diagram (Chapter 2), and novel supersymmetric vacua (Chapter 3), as realized in the D3/D5 probe brane systems. For further quantify various non-Fermi quantum liquids realized through the holographic probe brane construction, we also propose and verify the method to include the backreaction due to the probe brane at the leading order (Chapter 4), which is capable of detecting topological phase transitions.

There are various extensions towards better understanding of these novel quantum liquids. The direct continuation of Chapter 4 was to utilize the probe-brane entanglement entropy formula on the quantum liquid realized through the D3/D7 probe brane system at finite density and zero temperature. This work, in collaboration with Prof. Andreas Karch and Dr. Christoph F. Uhlemann, was released prior to this thesis [116]. Similar attempts should be possible to extend to the D3/D5 probe brane system, and hopefully further quantify the holographic model of Kondo effect [117]. However, there are also different approaches not addressed in this thesis: Gravity/Fluid duality, utilizing the notion of the hydrodynamical expansion with the EFT framework, provides us another handle to the non-equilibrium properties of those quantum liquids; We might also seek to invoke the ancient conformal bootstrap program to numerically investigate those properties from the field theory direction, as rekindled lately [118]. It is therefore quite an exciting endeavor to continue our journey of quantifying non-Fermi quantum liquids.

BIBLIOGRAPHY

[1] H.-C. Chang, "Minimal submanifolds asymptotic to $AdS_4 \times S^2$ in $AdS_5 \times S^5$," *JHEP*, vol. 1404, p. 037, 2014.

[2] H.-C. Chang and A. Karch, "Novel Solutions of Finite-Density D3/D5 Probe Brane System and Their Implications for Stability," *JHEP*, vol. 1210, p. 069, 2012.

[3] H.-C. Chang and A. Karch, "Entanglement Entropy for Probe Branes," *JHEP*, vol. 1401, p. 180, 2014.

[4] S. Weinberg, *The Quantum Theory of Fields, Volume 1: Foundations*. Cambridge University Press, 2005.

[5] A. Duncan, *The Conceptual Framework of Quantum Field Theory*. Oxford University Press, 2012.

[6] E. A. Calzetta and E. A. Hu, *Nonequilibrium Quantum Field Theory*. Cambridge University Press, 2008.

[7] J. Polchinski, "Effective field theory and the Fermi surface," 1992.

[8] D. H. Lyth and A. R. Liddle, *The Primordial Density Perturbation: Cosmology, Inflation and the Origin of Structure*. Cambridge University Press, 2009.

[9] M. Giovannini, *A Primer On The Physics Of The Cosmic Microwave Background*. World Scientific Publishing Company, 2008.

[10] A. Migdal, "Ancient History of CFT," *The 12th Claude Itzykson Meeting*.

[11] A. Dymarsky, Z. Komargodski, A. Schwimmer, and S. Theisen, "On scale and conformal invariance in four dimensions," 2013.

[12] J. Polchinski, *String Theory, Vol. 1 and Vol. 2*. Cambridge University Press, 1998.

[13] M. B. Green, J. H. Schwarz, and E. Witten, *Superstring Theory: Vol. 1 and Vol. 2*. Cambridge University Press, 1998.

[14] Blumenhagen, Ralph and Lüst, Dieter and Theisen, Stefan, *Basic Concepts of String Theory*. Springer, 2013.

[15] K. Becker, M. Becker, and J. H. Schwarz, *String Theory and M-Theory: A Modern Introduction*. Cambridge University Press, 2007.

[16] A. Giveon and D. Kutasov, "Brane dynamics and gauge theory," *Rev.Mod.Phys.*, vol. 71, pp. 983–1084, 1999.

[17] H. Georgi, *Weak Interactions and Modern Particle Theory*. Dover Publications, 2009.

[18] C. Burgess and G. Moore, *The Standard Model: A Primer*. Cambridge University Press, 2006.

[19] L. Ibanez and A. Uranga, *String Theory and Particle Physics: An Introduction to String Phenomenology*. Cambridge University Press, 2012.

[20] J. M. Maldacena, "The Large N limit of superconformal field theories and supergravity," *Adv.Theor.Math.Phys.*, vol. 2, pp. 231–252, 1998.

[21] E. Witten, "Anti-de Sitter space and holography," *Adv.Theor.Math.Phys.*, vol. 2, pp. 253–291, 1998.

[22] S. Gubser, I. R. Klebanov, and A. M. Polyakov, "Gauge theory correlators from noncritical string theory," *Phys.Lett.*, vol. B428, pp. 105–114, 1998.

[23] O. Aharony, S. S. Gubser, J. M. Maldacena, H. Ooguri, and Y. Oz, "Large N field theories, string theory and gravity," *Phys.Rept.*, vol. 323, pp. 183–386, 2000.

[24] J. Casalderrey-Solana, H. Liu, D. Mateos, K. Rajagopal, and U. A. Wiedemann, *Gauge/String Duality, Hot QCD and Heavy Ion Collisions*. Cambridge University Press, 2014.

[25] A. Cappelli, E. Castellani, F. Colomo, and P. Di Vecchia, *The Birth of String Theory*. Cambridge University Press, 2012.

[26] A. M. Polyakov, *Gauge Fields and Strings*. CRC Press, 1987.

[27] G. 't Hooft, "A Planar Diagram Theory for Strong Interactions," *Nucl.Phys.*, vol. B72, p. 461, 1974.

[28] R. F. Lebed, "Phenomenology of large N(c) QCD," *Czech.J.Phys.*, vol. 49, pp. 1273–1306, 1999.

[29] S. Coleman, *Aspects of Symmetry: Selected Erice Lectures*. Cambridge University Press, 1988.

[30] C. Johnson, *D-Branes*. Cambridge University Press, 2003.

[31] R. J. Szabo, *An Introduction to String Theory and D-Brane Dynamics*. World Scientific Publishing Company, 2004.

[32] P. West, *Introduction to Strings and Branes*. Cambridge University Press, 2012.

[33] J. Polchinski, "Introduction to Gauge/Gravity Duality," pp. 3–46, 2010.

[34] R. C. Myers, "Dielectric branes," *JHEP*, vol. 9912, p. 022, 1999.

[35] A. Karch and E. Katz, "Adding flavor to AdS / CFT," *JHEP*, vol. 0206, p. 043, 2002.

[36] A. Karch and L. Randall, "Open and closed string interpretation of SUSY CFT's on branes with boundaries," *JHEP*, vol. 0106, p. 063, 2001.

[37] O. DeWolfe, D. Z. Freedman, and H. Ooguri, "Holography and defect conformal field theories," *Phys.Rev.*, vol. D66, p. 025009, 2002.

[38] J. Casalderrey-Solana, H. Liu, D. Mateos, K. Rajagopal, and U. A. Wiedemann, "Gauge/String Duality, Hot QCD and Heavy Ion Collisions," 2011.

[39] T. Schafer and D. Teaney, "Nearly Perfect Fluidity: From Cold Atomic Gases to Hot Quark Gluon Plasmas," *Rept.Prog.Phys.*, vol. 72, p. 126001, 2009.

[40] D. Son, "Toward an AdS/cold atoms correspondence: A Geometric realization of the Schrodinger symmetry," *Phys.Rev.*, vol. D78, p. 046003, 2008.

[41] K. Balasubramanian and J. McGreevy, "Gravity duals for non-relativistic CFTs," *Phys.Rev.Lett.*, vol. 101, p. 061601, 2008.

[42] S. A. Hartnoll, C. P. Herzog, and G. T. Horowitz, "Holographic Superconductors," *JHEP*, vol. 0812, p. 015, 2008.

[43] S. A. Hartnoll, J. Polchinski, E. Silverstein, and D. Tong, "Towards strange metallic holography," *JHEP*, vol. 1004, p. 120, 2010.

[44] M. R. Gaberdiel and R. Gopakumar, "Minimal Model Holography," *J.Phys.*, vol. A46, p. 214002, 2013.

[45] R. Haag, *Local Quantum Physics: Fields, Particles, Algebras*. Springer, 1996.

[46] I. R. Klebanov and E. Witten, "AdS / CFT correspondence and symmetry breaking," *Nucl.Phys.*, vol. B556, pp. 89–114, 1999.

[47] K. Skenderis, "Lecture notes on holographic renormalization," *Class.Quant.Grav.*, vol. 19, pp. 5849–5876, 2002.

[48] T. Sakai and S. Sugimoto, "Low energy hadron physics in holographic QCD," *Prog.Theor.Phys.*, vol. 113, pp. 843–882, 2005.

[49] C. Graham and A. Karch *in preparation.*

[50] C. Fefferman and C. R. Graham, "Conformal invariants," *Astérisque, Numero Hors Serie*, vol. 95, 1985.

[51] I. Brunner, A. Hanany, A. Karch, and D. Lust, "Brane dynamics and chiral nonchiral transitions," *Nucl.Phys.*, vol. B528, pp. 197–217, 1998.

[52] J. M. Maldacena, "Wilson loops in large N field theories," *Phys.Rev.Lett.*, vol. 80, pp. 4859–4862, 1998.

[53] A. Karch, A. O'Bannon, and E. Thompson, "The Stress-Energy Tensor of Flavor Fields from AdS/CFT," *JHEP*, vol. 0904, p. 021, 2009.

[54] S. de Haro, S. N. Solodukhin, and K. Skenderis, "Holographic reconstruction of space-time and renormalization in the AdS / CFT correspondence," *Commun.Math.Phys.*, vol. 217, pp. 595–622, 2001.

[55] O. Aharony and D. Kutasov, "Holographic Duals of Long Open Strings," *Phys.Rev.*, vol. D78, p. 026005, 2008.

[56] J. Erdmenger, Z. Guralnik, and I. Kirsch, "Four-dimensional superconformal theories with interacting boundaries or defects," *Phys.Rev.*, vol. D66, p. 025020, 2002.

[57] D. Arean, A. V. Ramallo, and D. Rodriguez-Gomez, "Mesons and Higgs branch in defect theories," *Phys.Lett.*, vol. B641, pp. 393–400, 2006.

[58] D. Gaiotto and E. Witten, "Supersymmetric Boundary Conditions in N=4 Super Yang-Mills Theory," 2008.

[59] M. Ammon, J. Erdmenger, S. Lin, S. Muller, A. O'Bannon, *et al.*, "On Stability and Transport of Cold Holographic Matter," *JHEP*, vol. 1109, p. 030, 2011.

[60] C. G. Callan and J. M. Maldacena, "Brane death and dynamics from the Born-Infeld action," *Nucl.Phys.*, vol. B513, pp. 198–212, 1998.

[61] R. C. Myers and M. C. Wapler, "Transport Properties of Holographic Defects," *JHEP*, vol. 0812, p. 115, 2008.

[62] A. Karch and A. O'Bannon, "Holographic thermodynamics at finite baryon density: Some exact results," *JHEP*, vol. 0711, p. 074, 2007.

[63] A. Karch, D. Son, and A. Starinets, "Zero Sound from Holography," 2008.

[64] G. Gibbons, "Born-Infeld particles and Dirichlet p-branes," *Nucl.Phys.*, vol. B514, pp. 603–639, 1998.

[65] S. A. Hartnoll and L. Huijse, "Fractionalization of holographic Fermi surfaces," 2011.

[66] K. Jensen and A. O'Bannon, "Holography, Entanglement Entropy, and Conformal Field Theories with Boundaries or Defects," *Phys.Rev.*, vol. D88, no. 10, p. 106006, 2013.

[67] H. Casini, M. Huerta, and R. C. Myers, "Towards a derivation of holographic entanglement entropy," *JHEP*, vol. 1105, p. 036, 2011.

[68] S. Ryu and T. Takayanagi, "Holographic derivation of entanglement entropy from AdS/CFT," *Phys.Rev.Lett.*, vol. 96, p. 181602, 2006.

[69] T. Takayanagi, "Entanglement entropy from a holographic viewpoint," *Class.Quant.Grav.*, vol. 29, p. 153001, 2012.

[70] A. Karch and A. O'Bannon, "Metallic AdS/CFT," *JHEP*, vol. 0709, p. 024, 2007.

[71] S. Kachru, A. Karch, and S. Yaida, "Holographic Lattices, Dimers, and Glasses," *Phys.Rev.*, vol. D81, p. 026007, 2010.

[72] K. Jensen, S. Kachru, A. Karch, J. Polchinski, and E. Silverstein, "Towards a holographic marginal Fermi liquid," *Phys.Rev.*, vol. D84, p. 126002, 2011.

[73] K. Jensen, A. Karch, D. T. Son, and E. G. Thompson, "Holographic Berezinskii-Kosterlitz-Thouless Transitions," *Phys.Rev.Lett.*, vol. 105, p. 041601, 2010.

[74] M. Kulaxizi and A. Parnachev, "Holographic Responses of Fermion Matter," *Nucl.Phys.*, vol. B815, pp. 125–141, 2009.

[75] A. Karch, M. Kulaxizi, and A. Parnachev, "Notes on Properties of Holographic Matter," *JHEP*, vol. 0911, p. 017, 2009.

[76] M. Ammon, K. Jensen, K.-Y. Kim, J. N. Laia, and A. O'Bannon, "Moduli Spaces of Cold Holographic Matter," *JHEP*, vol. 1211, p. 055, 2012.

[77] M. Ammon, M. Kaminski, and A. Karch, "Hyperscaling-Violation on Probe D-Branes," *JHEP*, vol. 1211, p. 028, 2012.

[78] N. Ogawa, T. Takayanagi, and T. Ugajin, "Holographic Fermi Surfaces and Entanglement Entropy," *JHEP*, vol. 1201, p. 125, 2012.

[79] L. Huijse, S. Sachdev, and B. Swingle, "Hidden Fermi surfaces in compressible states of gauge-gravity duality," *Phys.Rev.*, vol. B85, p. 035121, 2012.

[80] M. Fujita, W. Li, S. Ryu, and T. Takayanagi, "Fractional Quantum Hall Effect via Holography: Chern-Simons, Edge States, and Hierarchy," *JHEP*, vol. 0906, p. 066, 2009.

[81] C. Hoyos-Badajoz, K. Jensen, and A. Karch, "A Holographic Fractional Topological Insulator," *Phys.Rev.*, vol. D82, p. 086001, 2010.

[82] T. Azeyanagi, A. Karch, T. Takayanagi, and E. G. Thompson, "Holographic calculation of boundary entropy," *JHEP*, vol. 0803, pp. 054–054, 2008.

[83] M. Chiodaroli, M. Gutperle, and L.-Y. Hung, "Boundary entropy of supersymmetric Janus solutions," *JHEP*, vol. 1009, p. 082, 2010.

[84] E. D'Hoker, D. Z. Freedman, S. D. Mathur, A. Matusis, and L. Rastelli, "Graviton and gauge boson propagators in AdS(d+1)," *Nucl.Phys.*, vol. B562, pp. 330–352, 1999.

[85] V. E. Hubeny, M. Rangamani, and T. Takayanagi, "A Covariant holographic entanglement entropy proposal," *JHEP*, vol. 0707, p. 062, 2007.

[86] M. Nozaki, T. Numasawa, A. Prudenziati, and T. Takayanagi, "Dynamics of Entanglement Entropy from Einstein Equation," 2013.

[87] G. Wong, I. Klich, L. A. P. Zayas, and D. Vaman, "Entanglement Temperature and Entanglement Entropy of Excited States," 2013.

[88] Y. Hikida, W. Li, and T. Takayanagi, "ABJM with Flavors and FQHE," *JHEP*, vol. 0907, p. 065, 2009.

[89] D. Gaiotto and D. L. Jafferis, "Notes on adding D6 branes wrapping RP**3 in AdS(4) x CP**3," *JHEP*, vol. 1211, p. 015, 2012.

[90] S. Hohenegger and I. Kirsch, "A Note on the holography of Chern-Simons matter theories with flavour," *JHEP*, vol. 0904, p. 129, 2009.

[91] M. Ammon, J. Erdmenger, R. Meyer, A. O'Bannon, and T. Wrase, "Adding Flavor to AdS(4)/CFT(3)," *JHEP*, vol. 0911, p. 125, 2009.

[92] K. Jensen, "More Holographic Berezinskii-Kosterlitz-Thouless Transitions," *Phys.Rev.*, vol. D82, p. 046005, 2010.

[93] O. Aharony, O. Bergman, D. L. Jafferis, and J. Maldacena, "N=6 superconformal Chern-Simons-matter theories, M2-branes and their gravity duals," *JHEP*, vol. 0810, p. 091, 2008.

[94] L. Randall and R. Sundrum, "A Large mass hierarchy from a small extra dimension," *Phys.Rev.Lett.*, vol. 83, pp. 3370–3373, 1999.

[95] L. Randall and R. Sundrum, "An Alternative to compactification," *Phys.Rev.Lett.*, vol. 83, pp. 4690–4693, 1999.

[96] W. Israel, "Singular hypersurfaces and thin shells in general relativity," *Nuovo Cim.*, vol. B44S10, p. 1, 1966.

[97] I. Kirsch and D. Vaman, "The D3 / D7 background and flavor dependence of Regge trajectories," *Phys.Rev.*, vol. D72, p. 026007, 2005.

[98] E. D'Hoker, J. Estes, and M. Gutperle, "Exact half-BPS Type IIB interface solutions. I. Local solution and supersymmetric Janus," *JHEP*, vol. 0706, p. 021, 2007.

[99] E. D'Hoker, J. Estes, and M. Gutperle, "Exact half-BPS Type IIB interface solutions. II. Flux solutions and multi-Janus," *JHEP*, vol. 0706, p. 022, 2007.

[100] O. Aharony, L. Berdichevsky, M. Berkooz, and I. Shamir, "Near-horizon solutions for D3-branes ending on 5-branes," *Phys.Rev.*, vol. D84, p. 126003, 2011.

[101] D. T. Son and A. O. Starinets, "Minkowski space correlators in AdS / CFT correspondence: Recipe and applications," *JHEP*, vol. 0209, p. 042, 2002.

[102] M. Turyn, "The graviton propagator in maximally symmetric spaces," *J.Math.Phys.*, vol. 31, p. 669, 1990.

[103] B. Allen and M. Turyn, "An evaluation of the graviton propagator in de Sitter space," *Nucl.Phys.*, vol. B292, p. 813, 1987.

[104] P. G. Freund and M. A. Rubin, "Dynamics of Dimensional Reduction," *Phys.Lett.*, vol. B97, pp. 233–235, 1980.

[105] O. DeWolfe, D. Z. Freedman, S. S. Gubser, G. T. Horowitz, and I. Mitra, "Stability of AdS(p) x M(q) compactifications without supersymmetry," *Phys.Rev.*, vol. D65, p. 064033, 2002.

[106] E. D'Hoker, D. Z. Freedman, and L. Rastelli, "AdS / CFT four point functions: How to succeed at z integrals without really trying," *Nucl.Phys.*, vol. B562, pp. 395–411, 1999.

[107] S. Ryu and T. Takayanagi, "Aspects of Holographic Entanglement Entropy," *JHEP*, vol. 0608, p. 045, 2006.

[108] L. Vanzo, "Black holes with unusual topology," *Phys.Rev.*, vol. D56, pp. 6475–6483, 1997.

[109] D. Birmingham, "Topological black holes in Anti-de Sitter space," *Class.Quant.Grav.*, vol. 16, pp. 1197–1205, 1999.

[110] R. Emparan, C. V. Johnson, and R. C. Myers, "Surface terms as counterterms in the AdS / CFT correspondence," *Phys.Rev.*, vol. D60, p. 104001, 1999.

[111] R. Emparan, "AdS / CFT duals of topological black holes and the entropy of zero energy states," *JHEP*, vol. 9906, p. 036, 1999.

[112] A. Lewkowycz and J. Maldacena, "Generalized gravitational entropy," 2013.

[113] D. Fursaev, "Quantum Entanglement on Boundaries," 2013.

[114] V. Iyer and R. M. Wald, "Some properties of Noether charge and a proposal for dynamical black hole entropy," *Phys.Rev.*, vol. D50, pp. 846–864, 1994.

[115] L.-Y. Hung, R. C. Myers, and M. Smolkin, "On Holographic Entanglement Entropy and Higher Curvature Gravity," *JHEP*, vol. 1104, p. 025, 2011.

[116] H.-C. Chang, A. Karch, and C. F. Uhlemann, "Flavored N=4 SYM – a highly entangled quantum liquid," 2014.

[117] J. Erdmenger, C. Hoyos, A. Obannon, and J. Wu, "A Holographic Model of the Kondo Effect," *JHEP*, vol. 1312, p. 086, 2013.

[118] S. El-Showk, M. F. Paulos, D. Poland, S. Rychkov, D. Simmons-Duffin, *et al.*, "Solving the 3D Ising Model with the Conformal Bootstrap," *Phys.Rev.*, vol. D86, p. 025022, 2012.